Univerzita Karlova

Přírodovědecká fakulta

Studijní program: Biochemie

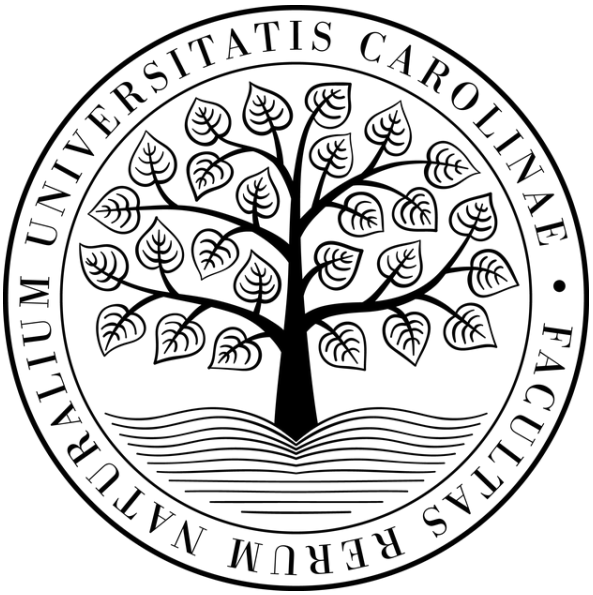

Bc. Gustav Kavale

Biologické vlastnosti konjugátů insulinu s N-acetylgalaktosaminem

Biological properties of insulin conjugates with N-acetylgalactosamine

Diplomová práce

Vedoucí závěrečné práce: RNDr Jiří Jiráček CSc.

Praha 2024

Prohlášení:

Prohlašuji, že jsem závěrečnou práci zpracoval samostatně a že jsem uvedl všechny použité informační zdroje a literaturu. Tato práce ani její podstatná část nebyla předložena k získání jiného nebo stejného akademického titulu. Text byl zpracován nástroji umělé inteligence, a to výhradně pro účely formátování textu. Žádná myšlenka, argument či závěr prezentovaný v této práci nebyl generován či jakkoli umělou inteligencí ovlivněn.

V Praze, *22.11.2024* Podpis:

Acknowledgement

Diplomová práce, která je finálním výsledkem akademického působení studentů magisterských oborů vysokých škol není jen nějaký kus papíru. Je to obrovitá míra vyvinuté práce a úsilí, je to projevem nasazení k výzkumu a poznání, je to několik těžkých měsíců, kdy se student musí obrnit a prokázat odolnost vůči tomu faktu, že mu nefunguje western-blot již po tisíci prvé, že ze záhadných důvodů nedochází k expresi receptorů v buněčných kulturách, či z toho, že už 3 dny neviděl světlo jiného původu než z monitoru. Proto zde chci poděkovat všem mým vedoucím a kolegům, kteří mě mou cestou za titulem doprovázeli, a i na úkor jejich nervů a mnohdy nadlidské trpělivosti mě vždy podporovali s úsměvem na líci.

Nejprve chci poděkovat rodičům, kteří mi poskytli teplo domova, poskytli mi zázemí a lásku za kterou jsem jim nesmírně vděčný. Bez těchto věcí bych určitě nezvládl dělat akademickou práci této úrovně a jistě bych nebyl schopen obhájit svoje znalosti, které jsem díky jejich zázemí nabyl.

V neposlední řadě chci poděkovat Univerzitě Karlově a Přírodovědecké fakultě. Těchto 6 let pro mě byl nepopsatelný zážitek, na který budu vzpomínat do konce svých dnů. UK mě hodně změnila k lepšímu. Při nástupu bych nikdy nečekal, že se zde naučím tolika chemických umů, poznal nespočetné množství přátel a kontaktů, které mi budou k užitku do konce života a naučil jsem se vědomostí, kterých budu používat ke kráse světa a zlepšení lidstva jako takového.

Téže bych chtěl poděkovat výzkumné skupině RNDr Jiřího Jiráčka a Ústavu Organické Chemie a Biochemie AVČR za zastřešení experimentů, výzkumu a celkového poznání, kterého mi bylo dopřáno.

Toto je poslední titul, který budu na PřF UK obhajovat. V přírodovědném odvětví však zůstanu do konce svého života neb je ze mě přírodovědec tělem i duší.

Tisíceré díky za vše vám všem.

This work was supported by the project National Institute for Metabolic and Cardiovascular Disease Research (Programme EXCELES, ID Project No. LX22NPO5104) - Funded by the European Union - Next Generation EU.

Abstract

Insulin is a key regulator of glucose metabolism in the body. Deficiencies in its function lead to a severe metabolic disorder known as diabetes mellitus. For some diabetics, daily insulin administration is the only way to survive. Currently, the only effective method for insulin administration is subcutaneous injection. However, subcutaneous (s.c.) injection results in delayed insulin action in the liver, leading to an imbalance in blood glucose levels and associated health complications. For this reason, significant efforts have been made to modify insulin in order to enhance its transport to the liver following subcutaneous administration. One way to improve the transport of substances from the blood to the liver is their conjugation with N-acetylgalactosamine (GalNAc). This strategy has been successfully used for the selective targeting of siRNA to liver cells. In this study, we aimed to verify the effectiveness of this strategy using insulin as an example. We prepared four insulin derivatives modified at positions B1 and B29 with mono-GalNAc or tri-GalNAc groups. All derivatives were tested for their ability to bind to insulin receptors. For further experiments, we selected the tri-GalNAcB1-insulin derivative, which was injected into mice. Shortly after the injection, samples of adipose and liver tissue were collected, and using electrophoresis and specific antibody detection, we examined differences in the activation (phosphorylation) of the insulin receptor and the proteins Akt and Erk. The results showed that insulin activated the insulin receptor and Akt protein more strongly in vivo than tri-GalNAcB1-insulin. We believe that the specific glycosylation of insulin does indeed lead to its interaction with the asialoglycoprotein receptor in the liver. However, this receptor rapidly internalizes the conjugated molecule and transports it to endosomes for degradation. While this mechanism is beneficial for siRNA transport, it is not suitable for insulin derivatives, which need to act on the cell surface. This study provided valuable insights into the chemical modifications of insulin and the biological properties of the resulting glycosylated conjugates in vivo.

Key words: *insulin, analogue, receptor, diabetes, hepatoselectivity, conjugates, insulin receptor, N-Ac galactosamine*

Abstrakt

Insulin je klíčovým regulátorem metabolismu glukózy v organismu. Nedostatky v jeho fungování vedou k závažnému metabolickému onemocnění zvanému diabetes mellitus. Pro část diabetiků je každodenní podávání insulinu jediným způsobem, jak zajistit přežití. V současnosti je jedinou efektivní metodou podávání insulinu subkutánní aplikace. Subkutánní (s.c.) podání však způsobuje zpožděné působení insulinu v játrech, což vede k nerovnováze hladin krevní glukózy a souvisejícím zdravotním komplikacím. Z tohoto důvodu bylo vyvinuto značné úsilí zaměřené na úpravu insulinu s cílem zvýšit jeho transport do jater po s.c. podání. Jedním ze způsobů, jak zlepšit transport látek z krve do jater, je jejich konjugace s N-acetylgalaktosaminem (GalNAc). Tato strategie je již úspěšně využívána pro selektivní cílení siRNA do jaterních buněk. V této práci jsme se rozhodli ověřit účinnost této strategie na příkladu insulinu. Připravili jsme čtyři deriváty insulinu, které byly modifikovány v pozicích B1 a B29 mono-GalNAc nebo tri-GalNAc skupinami. U všech derivátů jsme ověřili jejich schopnost vázat receptory pro insulin. Pro další experimenty jsme vybrali derivát tri-

GalNAcB1-insulin, který byl aplikován myším. Krátce po injekci byly odebrány vzorky tukové a jaterní tkáně, ve kterých jsme pomocí elektroforézy a detekce specifickými protilátkami zkoumali rozdíly v aktivaci (fosforylaci) insulinového receptoru a proteinů Akt a Erk. Z výsledků vyplývá, že insulin v in vivo podmínkách aktivuje insulinový receptor a protein Akt výrazně silněji než tri-GalNAcB1-insulin. Domníváme se, že specifická glykosylace insulinu skutečně podporuje jeho interakci s asialoglykoproteinovým receptorem v játrech. Tento receptor však navázaný konjugát rychle internalizuje a transportuje do endozomů k degradaci. Tento mechanismus, přestože je výhodný pro transport siRNA, není vhodný pro deriváty insulinu, které vyžadují působení na povrchu buňky. Tato studie přinesla cenné poznatky o chemických modifikacích insulinu a biologických vlastnostech výsledných glykosylovaných konjugátů in vivo.

LIST OF ABBREVIATIONS AND SYMBOLS

AA - Amino Acid

ACN - Acetonitrile

AKT - A kinase involved in signaling pathways (Protein Kinase B)

ASGP(R) – Asialoglycoprotein (receptor)

DMEM - Dulbecco's Modified Eagle's Medium (a cell culture medium)

DOI - Des-octapeptide Insulin

EDTA - Ethylenediaminetetraacetic Acid (a chelating agent)

eWAT - Ependymal White Adipose Tissue

ERK - Extracellular Signal-Regulated Kinase

GalNAc - N-Acetylgalactosamine

GLUT - Glucose Transporter

HBB - Hemoglobin Subunit Beta

HBTU - O-Benzotriazol-1-yl-N,N,N′,N′-tetramethyluronium hexafluorophosphate (a reagent used in peptide chemistry)

HI - Human Insulin

HPLC - High-Performance Liquid Chromatography

IN - Insulin

INS - Insulin Gene

IOCB - Institute of Organic Chemistry and Biochemistry (Czech Academy of Sciences)

IRS - Insulin Receptor Substrate

MAPK - Mitogen-Activated Protein Kinase

MEK - MAPK/ERK Kinase

PI3K - Phosphoinositide 3-Kinase

Raf - Proto-Oncogene Serine/Threonine-Protein Kinase

Ras - Rat Sarcoma (a GTPase protein involved in cell signaling pathways)

TFA - Trifluoroacetic Acid

COMMON LATIN ABBREVIATIONS

e.g. “exempli gratia.” for example
in vitro performed in a test tube, culture dish, or elsewhere outside a living organism
in vivo performed in a living organism.
et al. “et alii” and others

1. Introduction

1.1 Insulin

Insulin is a hormone peptide composed of 51 amino acids (AA) divided into 2 separate chains (A-chain and B-chain) connected via 2 disulphide bridges and with the third disulphide in the A-chain (Figure 1).

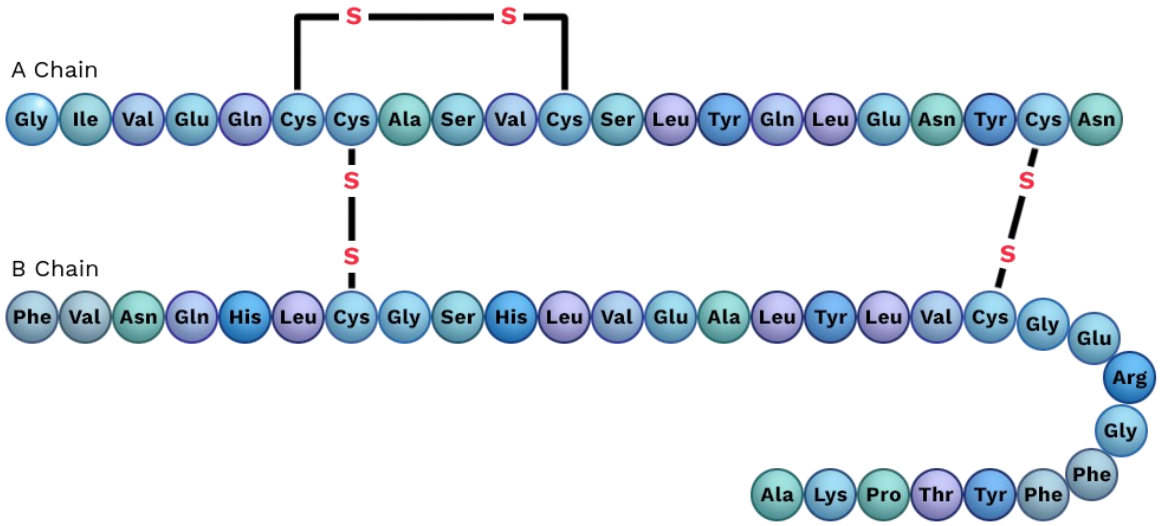

Figure 1 The A and B chains of insulin are linked together by disulfide bonds [1].

Insulin is the main anabolic hormone present in human body, and it has a huge effect on metabolism of sugars, fats and proteins. The most important action of insulin is in lowering blood sugar levels via translocation of glucose transporter (GLUT4) on the surface of adipose and muscle cells that enables uptake of glucose into the intracellular space of adipose and muscle tissues thus enabling its metabolizing [2]. In hepatocytes it also triggers synthesis of glycogen, thus storing blood sugar for further use. Another important function of insulin in liver is inhibition of gluconeogenesis and glycogenolysis [3].

Insulin is produced by pancreatic cells, to be specific by β cells of pancreatic islets of Langerhans [4], and it is encoded in humans by insulin gene (INS) [5].

1.1.1 Mechanism of insulin action

Insulin is an anabolic peptide hormone secreted by the pancreatic β-cells to the bloodstream in response to elevated glucose levels. Its counter player hormone is glucagon that is also released from pancreas but has opposite effects glucose metabolism (Figure 2).

Insulin acts through binding to and activation of insulin receptors located on the membranes of target cells [6]. Insulin secreted from pancreas through portal vein primarily targeting the liver, where it promotes glucose storage as glycogen and reduces glucose production through inhibition of gluconeogenesis and glycogenolysis. The remaining insulin (about 50%) leaves the liver and reaches skeletal muscle and fat tissue, where it stimulates glucose uptake by triggering the translocation of GLUT4 transporters [7]. Insulin also affects β-cells, brain cells, and most other cell types, where it exerts a range of pleiotropic effects [8].

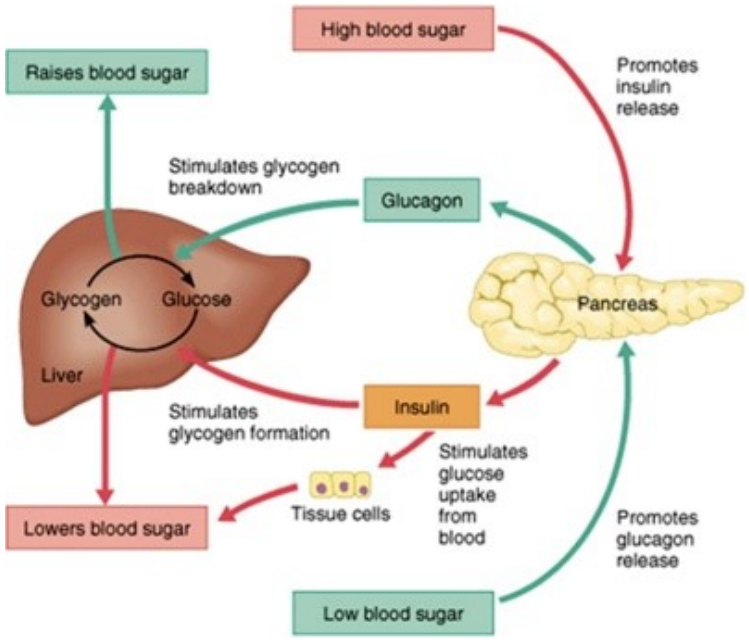

Figure 2 General principles of insulin and glucagon action on the metabolism of saccharides [9].

Insulin signalling primarily follows two key pathways originating from the activation of the insulin receptor-IRS (insulin receptor substrate) node [10]. These are the phosphatidylinositol 3-kinase (PI3K, a lipid kinase)/AKT (also known as PKB or protein kinase B) pathway and the Raf/Ras/MEK/MAPK (mitogen-activated protein kinase, also known as ERK or extracellular signal-regulated kinase) pathway. The PI3K pathway is mainly responsible for the metabolic effects of insulin and operates exclusively through IRS. In contrast, the MAPK pathway originates from both IRS and Shc and is involved in regulating gene expression. Together with the PI3K pathway, it plays a role in controlling cell growth ("mitogenesis") and differentiation (Figure 3).

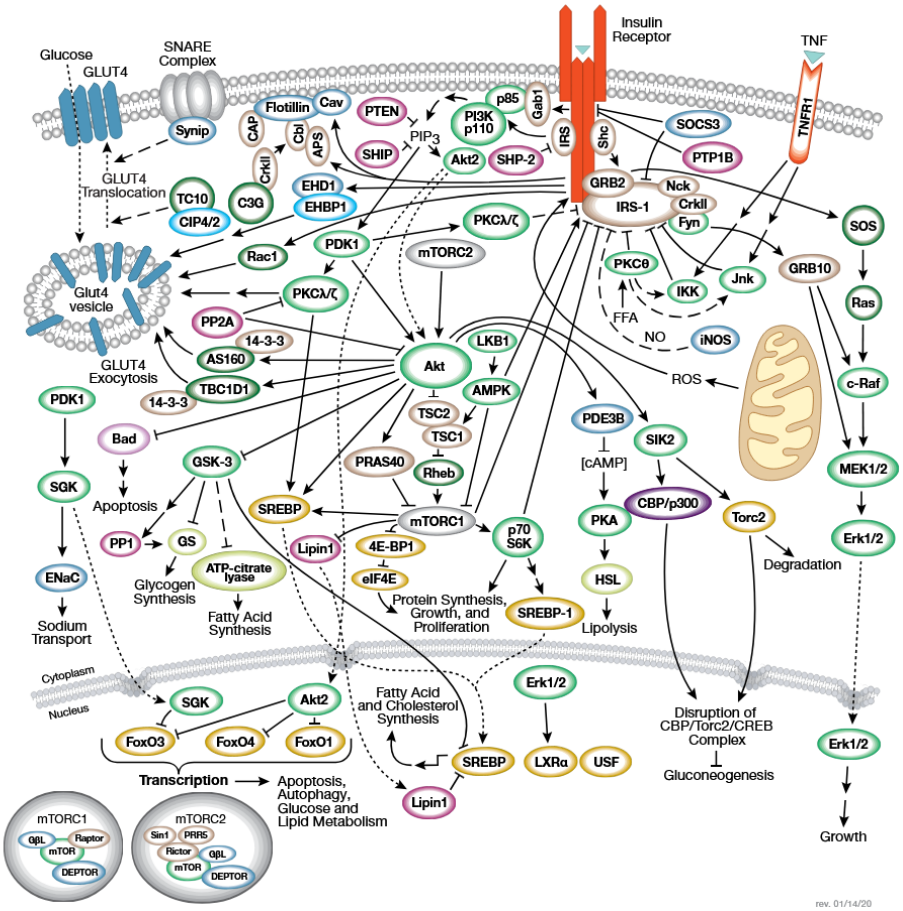

Figure 3 A overview of inulin: insulin receptor signalling. [11]

1.2 Insulin receptor and its isoforms

Insulin exerts its essential effects by binding to the insulin receptor (IR), a large transmembrane glycoprotein that exists in two isoforms, IR-A and IR-B, produced through alternative splicing of the IR gene [12]. The key difference between these isoforms is a 12-amino acid insertion found at the C-terminus of the extracellular α-subunit in IR-B but absent in IR-A (Figure 4).

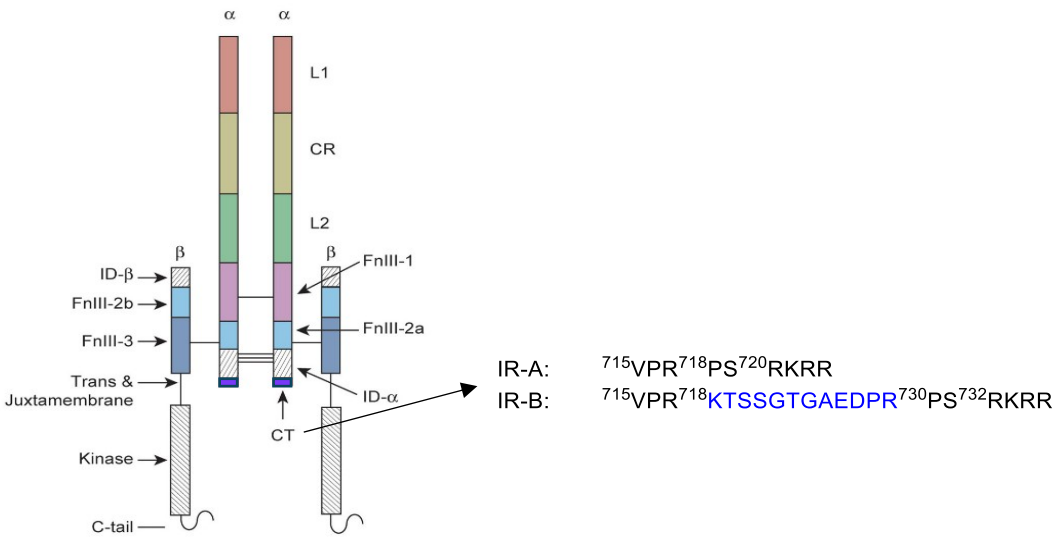

Figure 4. Schematic structure of the insulin receptor isoforms IR-A and IR-B that differ in the C-terminal part of the α-subunit (α-CT peptide). α-CT peptide of IR-B contains 12 extra amino acids (in blue). Created in the laboratory of Jiří Jiráček in IOCB.

This differential region, called the α-CT peptide, spans residues 700−723 in IR-A and 700−735 in IR-B. While insulin binds to both isoforms with similar affinity, insulin-like growth factors (IGF) 1 and 2, members of the insulin-like protein family, bind IR-B with significantly lower affinity compared to IR-A [13].

The IR isoforms are distributed differently across tissues [14]. IR-B predominates particularly in hepatocytes (over 95%) and is also highly expressed in skeletal muscles and subcutaneous fat (both around 70% IR-B). In contrast, IR-A is primarily expressed in the brain, lymphatic tissues, and during embryonic development. IR-A, unlike its counterpart IR-B, seems to be a crucial part in insulin and IGF-2 signalling in tumours and cancer cells alike. Generally speaking, IR-B receptor could be addressed as the "metabolic" form of the receptor, while IR-A receptor could be associated with "mitogenic" effects, due to its role in proliferation. Some studies suggest that IR-A and IR-B differ in their rates of insulin association and dissociation, though it remains unclear if insulin activates distinct cellular proteins depending on the isoform

it binds. The differential tissue distribution of these isoforms may underlie their primarily metabolic and mitogenic roles, respectively.

Binding of insulin to dimeric insulin receptor triggers conformational change that results in mutual approaching of the transmembrane and intracellular receptor domains and autophosphorylation of several tyrosine residues in the IR intracellular tyrosine-kinase domains [15]. The phosphorylation signal is then transduced to other intracellular proteins and signalling cascades (Figures 3).

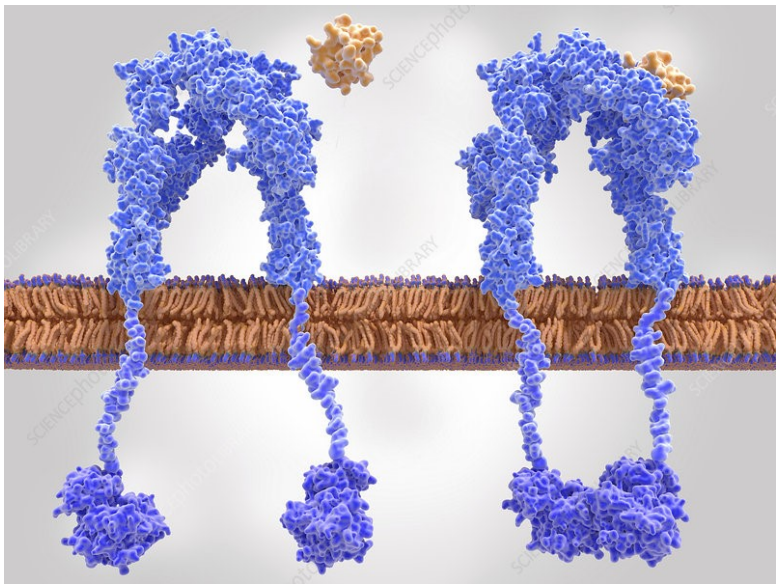

Figure 5 Visual representation of insulin receptor inactive form (left) and activated insulin receptor (right) [16].

1.3 Current insulin therapy and its drawbacks

The lives of millions of diabetic patients around the world are being saved today through the daily administration of insulin but mainly of its derivatives, so-called analogues [16]. Insulin analogues are covalently modified insulin with properties that bring patients more comfort that treatment with human insulin. The problem in not in insulin itself but in a way of its administration to patients [17].

Insulin is a small protein and, as such, cannot be administered orally. For this reason, insulin is administered subcutaneously to patients. However, with this type of administration, insulin reaches the liver with a delay compared to the normal physiological secretion from the pancreas [18]. This delay also leads to delayed inhibition of liver glucose production, resulting in imperfect regulation of blood glucose levels in patients, which can lead to health

complications (Figure 5). For this reason, efforts have been made to develop hepatoselective insulin, i.e., an insulin analogue that would reach the liver faster than human insulin after subcutaneous administration [19].

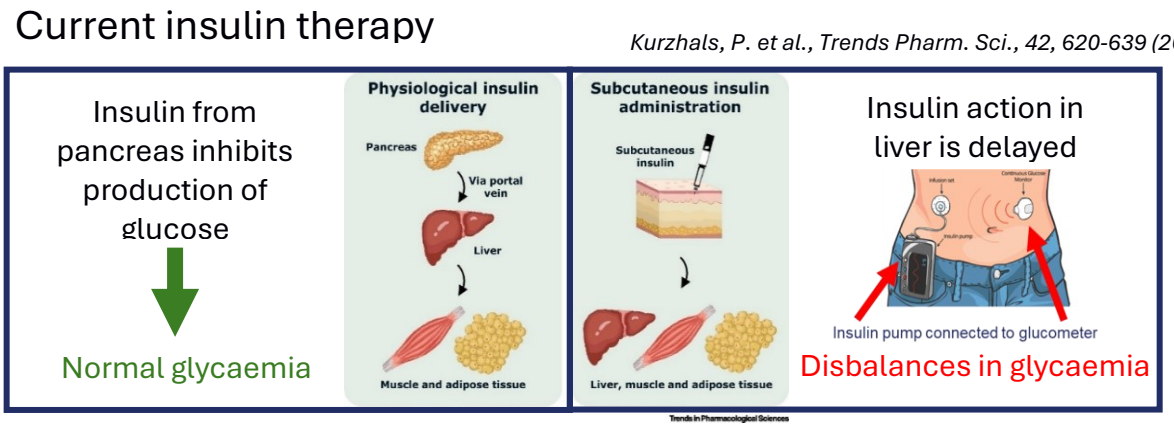

Figure 6 Representation of main drawbacks of current insulin therapy [19]

1.4. Insulin analogues with hepatopreferential action

Few insulin analogues were designed and studied to have hepatopreferential action *in vivo*. Their hepatoselectivity was based on different principles.

The fast-acting insulin analogue LY2605541 (peglispro), developed by Eli Lilly, involves a substitution of ProB28 with LysB29 and the addition of a 20 kDa polyethylene glycol moiety [20]. The increased molecular size of this analogue alters its tissue distribution, favoring the liver over peripheral tissues. This size increase also results in slower subcutaneous absorption and a significantly reduced glomerular filtration rate, both of which contribute to a notably prolonged half-life of the peptide. Clinical trials of insulin peglispro confirmed the preclinical pharmacokinetics, demonstrating a sustained glucose-lowering effect that lasted up to 36 hours. A distinguishing characteristic of this insulin analogue was its hepatoselective action, which was confirmed by euglycaemic clamp studies in dogs. Subcutaneous administration of insulin peglispro showed a preferential effect on the liver, evidenced by a shift from net hepatic glucose output to peripheral glucose utilization. However, in 2015, Eli Lilly halted the development of peglispro after Phase III trials revealed elevated alanine

transaminase levels and increased liver fat, which were identified as potentially harmful side effects. [21]

In the context of hepatoselectivity, isoform-specific insulin analogues could be also valuable for investigating the functions of IR-A and IR-B in different tissues. Insulin analogues with a binding preference for IR-B (and importantly lower binding affinity for IR-A) could enhance hepatic bioactivity in vivo and potentially offer a more physiological treatment profile for diabetes. Hypothetically, IR-B specific insulin could be less trapped after such injection by IR-A than human insulin and more of it could reach liver. Moreover, higher levels of circulating insulin have been associated with increased cancer risk and progression in epidemiology studies [22] and it is IR-A that is mainly associated with cancer issues, IR-B-specific insulin analogues could find application in safer manner of treatment of diabetes. On the other hand, insulins more specific for IR-A (prevalent in the brain) and with reduced binding to IR-B (prevalent in the liver), could be interesting for safer (with a lower risk of systemic hypoglycaemia) treatment of neurological disorders linked to insulin deficiency in the brain, where insulin can be locally administered by intranasal application [23].

Novo Nordisk A/S focused on development of IR-B specific insulin analogue as, due to predominant expression of IR-B in liver, it could be also hepatoselective [20]. The Novo Nordisk team developed [HisA8,AsnB25,GluB27,desThrB30]-insulin analogue with about 30 % binding affinity for IR-B (related to the binding affinity of human insulin) and about 10 % for IR-A (IR-B/IR-A binding affinity ratio of about 3). The same team also reported [GlnA18,desThrB30]-insulin analogue having GlyA1 and LysB29 residues connected by the VGLSSGQ sequence and with 55% binding affinity for IR-A and 10% binding affinity for IR-B (IR-B/IR-A ratio of about 0.18). Both analogues were tested for their physiological effects in rats, which have more than 90% IR-B in hepatocytes and in fat cells and more than 90% IR-A in muscle cells. The IR-A more specific analogue had a higher potency (stimulation of glycogen synthesis) in rat muscles than IR-B specific insulin. On the other hand, the IR-B more specific analogue had higher potency in hepatocytes and adipocytes (via the stimulation of glycogen accumulation and lipogenesis, respectively) than its IR-A more specific counterpart. Interestingly, Novo Nordisk has not further exploited these interesting results. Neverthelles, these results indicate that insulins with a relatively moderate receptor isoform binding specificity can induce tissue-specific effects [14].

The research group of Jiří Jiráček in IOCB has developed an insulin analogue LZ-162 (AlaB29,GluB31-carboxymide insulin) that has about 138 % of binding affinity of human insulin on IR-B and about 44% binding affinity of human insulin on IR-A. LZ-162 had IR-B

selectivity similar to Novo Nordisk [HisA8,AsnB25,GluB27,desThrB30]-insulin analogue, but is more potent. LZ-162 showed higher efficiency in insulin tolerance test in mice [21]. Currently, LZ-162 is tested in mice to show its potential tissue specificity compared to human insulin.

1.5 GalNAc/ASGPR system for liver targeting

Another strategy for liver targeting of drugs employs *N*-Acetylgalactosamine (GalNAc)/ asialoglycoprotein receptor (ASGPR) system.

N-Acetylgalactosamine (GalNAc) is amino saccharide derived from galactose. Its main biological role in organism is act as antigen structure in blood group A. *N*-Acetylgalactosamine is necessary for intercellular communication and is concentrated in sensory nerve structures of both humans and animals [24]. Derivates of GalNAc and tri-GalNAc have showed the ability to target hepatocytes and to increase bioavailability and delivery of conjugated siRNAs [24]. Three GalNAc groups (tri-GalNAc) in one molecule have proven to have better pharmacodynamic properties then one GalNAc moiety. Use of tri-GalNAc in siRNA delivery systems enhances targeting, improves cellular uptake, and leads to effective therapeutic responses. This mechanism of targeting is attributed to the ASGPR binding. ASGPR is located predominantly on hepatic cells and its main function is in catabolism of glycoproteins delivering them to endosomes. GalNAc-conjugated siRNAs are designed to target liver-derived diseases after selective targeting of hepatocytes in the liver. Following subcutaneous administration, GalNAc moieties are rapidly cleaved by β-N-acetylglucosaminidase during endolysosomal trafficking. Subsequently, the linker structure is further metabolized by amidases in hepatocytes [24] via (Figure 7). This mechanism seems to be general for different conjugates with siRNA.

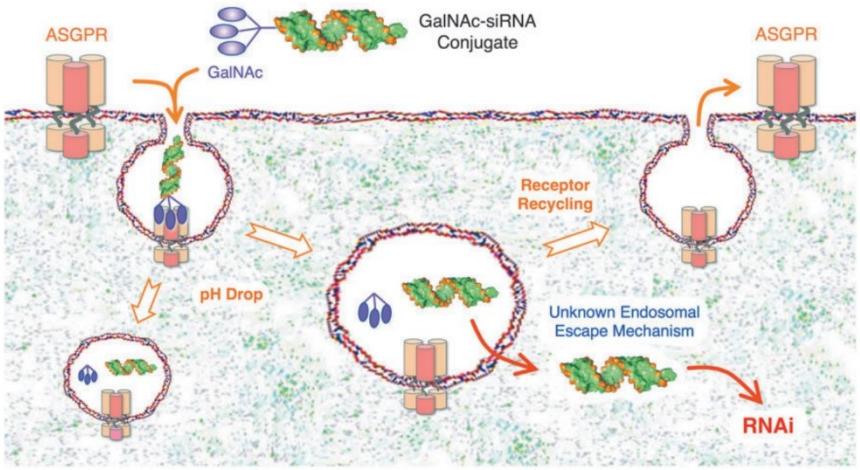

Figure 7 Delivery of GalNAc-siRNA conjugates into hepatocytes. Due to a pH drop, GalNAc-siRNA conjugates are released from ASGPR into the lumen of the endosome, and ASGPR recycles back to the hepatocyte surface [24].

In this study, we hypothesized that covalent conjugation of insulin to GalNac group(s) could alter the pharmacokinetic and pharmacodynamic properties of the hormone, leading to enhanced hepatic action after administration to mice, compared to human insulin. If this strategy proves successful or promising, the next step could be the conjugation of IR-B-specific insulin (e.g., LZ-162) to GalNac, potentially resulting in an even more hepatopreferential insulin derivative.

2. Aims of the work

The aim of this master diploma thesis was to evaluate a biological potential of insulin conjugates with GalNAc moiety. The biological effects of the conjugates have been tested both *in vitro* in cell cultures and *in vivo* in animals.

Specific aims:

1. Prepare insulin conjugates with mono-GalNAc moiety attached either to B29 or B1 position in insulin.
2. Prepare insulin conjugates with tri-GalNAc moiety attached either to B29 or B1 position in insulin.
3. Determine binding affinities of conjugates for IR isoforms in transfected fibroblasts.
4. Determine if the selected conjugate can elicit tissue-specific effects in animals in comparison with human insulin.

3. Experimental part

3.1 Materials and instruments

3.1.1 Chemicals

^{125}I-TyrA14 human insulin	SigmaAldrich, Germany
1,4-butanediol	SigmaAldrich, Germany
4-ethynylbenzaldehyde	SigmaAldrich, Germany
Acetonitrile	VWR chemicals, USA
Bovine serum albumine	Biosera, France
Ca(Ac)2	Verkon, Czech Republic
$CuSO_4 \cdot 5H_2O$	Verkon, Czech Republic
Diethyl ether	Lach-Ner, Czech Republic
Dimethylacetamide	SigmaAldrich, Germany
Dimethylformamide	VWR chemicals, USA
Dimethyldioxirane	SigmaAldrich, Germany
Dimethylsulfoxide	Sigma Aldrich, Germany
Dichloromethane	SigmaAldrich, Germany
Dichlormethan	Penta, Czech Republic
DMSO	SigmaAldrich, Germany
Ethylenediaminetetraacetic acid	SigmaAldrich, Germany
FBS	Biosera, France
Fmoc-Prg	SigmaAldrich, Germany
Fmoc-protected amino acids	SigmaAldrich, Germany
HBB	Biosera, France
HBTU	Iris Biotech, Germany
Hydroxybenzotriazole	Glenham, UK
Laemmli Sample buffer 4x	Bio – Rad laboratories, USA
L-glutamine	Biosera, France
N-methylmorpholine	SigmaAldrich, Germany
N,N-Diisopropylcarbodiimide	AK Scientific, USA
N,N-Diisopropylethylamine	TCI, USA
Penicillin-Streptomycin	Merck, Germany
Phosphate buffer saline	Biosera, France
Piperidine	Iris Biotech, Germany
Protease Inhibitor Cocktail (P8340)	Sigma Aldrich, Germany
RIPA, Lysis Buffer	Merck, Germany
Sodium Ascorbate	Merck, Germany
Sodium cyanoborohydride	SigmaAldrich, Germany
tert-butyldimethylsilyl chloride	Penta s.r.o., Czech Republic
Trifluoroacetic acid	Fluorochem, UK
Tri-GalNAc and Mono-GalNAc azides	SigmaAldrich, Germany
Triisopropylsilane	SigmaAldrich, Germany
Tris/HCl buffer	Biogen, Czech Republic
Trypsin/EDTA	Merck, Germany
Urea	SigmaAldrich, Germany
Wang resin	SigmaAldrich, Germany

Table 1: Primary and secondary antibodies used for detection of protein structures. Dilutions shown are in 1% BSA in T-TBS.

Detected protein/structure	Antibody name	Dilution	Organism of origin	Mr Range
Primar antibodies detecting phosphorylated protein				
pAkt	Phospho-Akt (Thr308) (C31E5E) Rabbit mAb, **Cell Signaling Technology, USA**	1:1000	Rabbit	>75 kDa
pErk	Phospho-p44/42 MAPK (Erk1/2) (Thr202/Tyr204) (E10) Mouse mAb, **Cell Signaling Technology, USA**	1:2000	Mouse	> 50 kDa
pTyr 1162/1163 IR / pTyr 1135/1136 IGF1R	Phospho IGF1R ß (Tyr1135/1136)/ InsR ß (19H7) Rabbit mAb, **Cell Signaling Technology, USA**	1:1000	Rabbit	<75 kDa
GAPDH	GAPDH (D4C6R) Mouse mAb, **Cell Signaling Technology, USA**	1:1000	Mouse	> 50 kDa
Secondary antibodies				
Antibodies aimed agains primary antibodies of rabbit origin	Anti-Rabbit IgG (whole molecule) - Peroxidase antibody produced in goat **Sigma-Aldrich, Germany**	1:80000	Goat	
Antibodies aimed agains primary antibodies of mouse origin	Anti-Rabbit IgG (whole molecule) - Peroxidase antibody produced in rabbit **Sigma-Aldrich, Germany**	1:20000	Rabbit	

3.1.2 Instruments

Spyder Mark IV Multiple Peptide Synthesizer	AAPPTec LLC
Waters HPLC system	Waters Corporation
Waters™ e2695 Separations Module	Waters Corporation
24-well plates	Schoeller
Column YMC-Triart C4, 250 x 4.6 mm	YMC
Column Phenomenex Luna C18, 250 x 21 mm	Phenomenex Inc.
Column Nucleosil C18, 250 x 4 mm	Macherey-Nagel GmbH
Column Macherey-Nagel C18, 250 x 10 mm	Macherey-Nagel GmbH
Column Vydac C4 214TP, 250 x 10 mm	Grace/Vydac
Column TriArt C4, 250 x 4 mm	YMC
LTQ Orbitrap XL	Waltham
Mass spectrometer MALDI Ultraflex	Bruker
EVETM Automated Cell Counter	NanoEnTek
2470 WIZARD^2 Automatic Gamma Counter	PerkinElmer

3.2 Synthesis of PrgB29-insulin analogue

3.2.1 Solid phase peptide synthesis

Octapeptide GFFYTP(Prg)T representing amino acids B23-B30 of human insulin and with LysB29 replaced by L-propargylglycine (Prg) was synthetized by the solid phase synthesis on Fmoc-Thr(tBu)-preloaded Wang resin. The synthesis was performed on Spyder Mark IV Multiple Peptide Synthesizer (developped in IOCB) via Fmoc synthesis by a standard protocol for solid phase synthesis of peptides used in the laboratory of Jiří Jiráček in IOCB [26].

Briefly, 0.1 mmol of Fmoc-Thr(tBu)-resin (0.65 mmol/g) was placed to a 12 ml syringe equipped with a porous Teflon frit. The syringe was placed to a reactor compartment of peptide synthesizer and swelled in DMF. The deprotection of the N-terminal Fmoc group was done with two additions of 20% piperidine in DMF (2 ml for 2 and 20 min). Fmoc-amino acids (eventually side chain protected) were added in two couplings, the first with 3 molar equivalents (0.75 ml of 0.4 M) of Fmoc-amino acid), 0.28 molar equivalents of 0.4 M HBTU (0.71 ml) and 5.7 molar equivalents of DIPEA (0.57 ml of 1 M) for 1h follow by the second coupling with 3 molar equivalents (0.75 ml of 0.4 M) of Fmoc-amino acid) and 4.4 equivalents of 1 M DIC (1 ml) also for 1h. All reagent and amino acids were dissolved in DMF. After couplings and Fmoc deprotection, the resin was washed with 5x 2.5 ml of DMD for 5 x 1 min. After the synthesis, the resin was washed with dichloromethane and dried.

The peptide was cleaved from resin with 5 ml of 95% TFA, 2.5% water and 2.5% TIS for 2h. The peptide was precipitated from a cleavage mixture with 45 ml of cold diethyl ether and dried. The peptide was purified via use of RP-HPLC (column Phenomenex Luna C18, 250 x 21 mm) using two mobile phases; A – 0,1% TFA in dH_2O and B – 80% ACN with 0,1% TFA also in dH_2O. The linear gradient of 10% B to 100% B in 30 min at 9 ml/ml was used and presence of the peptide was monitored by at 218 nm and 258 nm. The identity of peptide was confirmed by mass spectrometry mass spectrometry. The final purity of product was confirmed via analytical RP-HPLC (Nucleosil C18 250 x 4 mm) using the same conditions but at 1 ml/min.

3.2.2 Enzymatic semisynthesis of PrgB29-insulin

The conjugation of GFFYTP(Prg)T with des(B23-B30)-shortened insulin (DOI) was catalyzed by trypsin [26]. The octapeptide (19.3 mg, 20.8 μmol) was added to DOI (15 mg/3.08 μmol) and dissolved in a mixture of 140 μl DMA (35% v/v), 140 μl 1,4-butanediol (35 % v/v) and 30% (v/v) Tris/HCl (0.2M, pH 8), 10 mM $Ca(Ac)_2$ and 1 mM EDTA. After dissolving all

compounds, the pH was adjusted by N-methylmorpholine to about 7 (pH paper). This final mixture was left to shake for 18 hours and samples were taken from mixture for further examination every 2 hours.

The product was purified on Macherey-Nagel C18 column (250 x 10 mm) using a system of two mobile phases; A – 0,1% TFA in H_2O and B – 80% ACN with 0,1% TFA also in H_2O. The following gradient was used: 0 min 10% B, 1 min 35%, 21 min 45% B, 34 min 55% B, 36 min 90% B at 3 ml/ml was used and presence of the peptide was monitored by at 218 nm and 258 nm. The identity of final product newly formed B29 alkyne analogue was confirmed by mass spectrometry and by analytical RP-HPLC as described above.

The structure of the alkyne amino acid (Prg) at the position B29 of insulin is shown in Figure 8A.

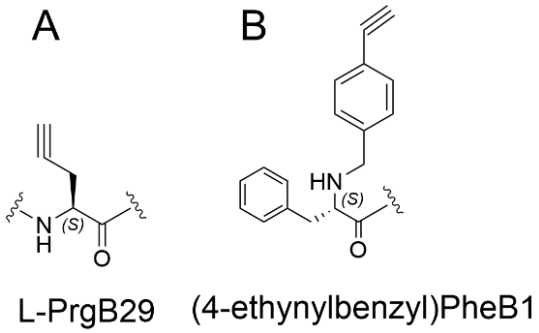

Figure 8. A Structure of L-propargylglycine (Prg) at the position B29 of human insulin. B. PheB1 of human insulin with (4-ethynylbenzyl)phenylalanine at the position B1.

3.3 Synthesis of (4-ethynylbenzyl)B1-insulin analogue

3.3.1 Preparation of (4-ethynylbenzyl)B1-insulin

To prepare insulin (4-ethynylbenzyl) B1-insulin; 40 mg of zinc-free human insulin was weighed and added to 2 ml of citric acid buffer (pH = 5.5-6.0, 25 mM) with dissolved 5 equivalents of reducing agent $NaBH_3CN$ (2.2 mg). Then 2 equivalents of 4-ethynylbenzaldehyde (2.0 mg) dissolved in 140 µl of dimethylsulfoxide (DMSO) were added to the 2 ml of homogeneous insulin suspension. The reaction was stirred on rolling shaker for 6 hours at room temperature. After the time elapsed the reaction progress was monitored by liquid chromatography conjugated with mass spectrometry (LC-MS). To complete the conversion, the reaction mixture was put and stirred in the cold room overnight. The following day, the progress was checked once again, and the reaction was stopped by putting the mixture into −80°C freezer until the purification. The crude purification was performed on reverse phase high pressure liquid chromatography (HPLC) system with C4 column (Vydac 214TP 250 x 10 mm) using mobile

phase A (0.1% trifuoroacetic acid in water) and B (80% acetonitrile with 0.1% trifluoroacetic acid in water). The product was purified using the following gradient of 10% B to 100% B in 30 min at 3 ml/ml and monitored by at 218 nm and 258 nm. The identity of peptide was confirmed by mass spectrometry mass spectrometry. The final purity of product was confirmed via analytical RP-HPLC (TriArt C4 column, 250 x 4 mm) using the same conditions but at 1 ml/ml.

The structure of alkyne functionalized amino acid B1 in insulin is shown at the position B29 of insulin is shown in Figure 8B.

.

3.4 Click-reactions with GalNAc moieties

The conjugates of human insulin with were prepared by Cu^{1+}-catalysed cycloaddition of azides and terminal alkynes ("click" reaction that provides a covalent 1,2,3-triazole bond, Figure 10) from respective insulin precursor with alkyne group at the position B29 or B1 and mono- or tri-GalNac derivatives functionalized with azido group. The protocol published by Viková et. al [25] was used for the click reaction.

3.4.1 Preparation of of mono-GalNAcB29-insulin

Insulin-B29-alkyne (1 mg, 1 equivalent) was weighed into a 1.5 mL Eppendorf, and 1 M urea in H_2O was added to prepare a 1 mM solution. To this, 0.1 M $CuSO_4 \cdot 5H_2O$ (12 equivalents) in H_2O was added, followed by the addition of 0.1 M mono-GalNAc azide (3 equivalents) in DMSO. The structure of mono-GalNAc azide is shown in Figure 9. Finally, a 0.1 M sodium ascorbate solution (14 equivalents) in H_2O was added. The reaction mixture was stirred at 25°C at 400 rpm for 24 hours to 2 days, protected from light, and monitored by RP-HPLC.

The peptide was purified using a Waters HPLC system (Waters 600 with a 2487 Dual λ Absorbance Detector) and a YMC-Triart Bio C4 column (250 x 4.6 mm, 5 µm). The flow rate was set to 1 mL/min, with the following gradient: t = 0 min, 10% B; t = 30 min, 100% B; t = 31 min, 10% B. Solvent A consisted of 0.1% TFA in H_2O, and solvent B was 80% acetonitrile (ACN) in A (v/v). The peptide was detected at 218 nm.

The purity of the peptide was assessed by HPLC using a Waters™ e2695 Separations Module with a 2489 UV/Vis Detector, employing the same column, flow rate, gradient, and solvents as previously described. The peptide's molecular weight was confirmed by high-resolution mass spectrometry (HRMS) using an LTQ Orbitrap XL (Thermo Fisher Scientific, Waltham, MA).

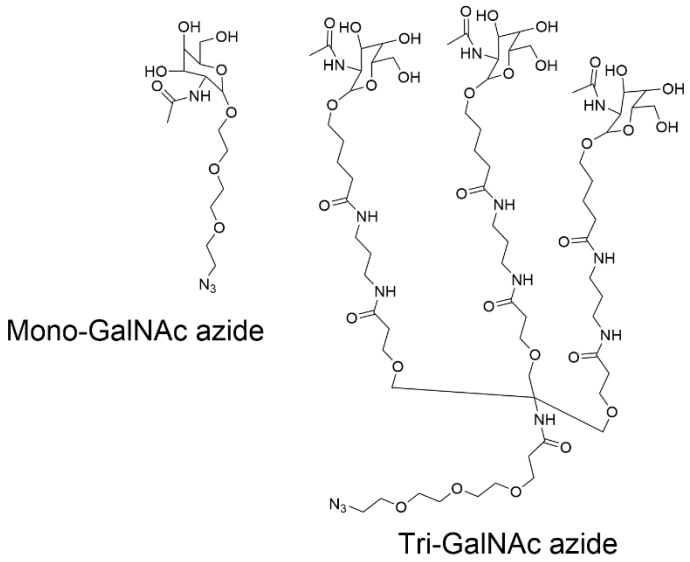

Figure 9, The structures of mono-GalNAc and tri-GalNAc azides used for derivatization of B29 and B1 alkyne insulins.

3.4.2 Preparation of mono-GalNAc B1-insulin analogue

(4-ethynylbenzyl)B1-insulin (1 mg, 1 equivalent) was weighed into a 1.5 mL Eppendorf, and 1 M urea in H_2O was added to prepare a 1 mM solution. To this, 0.1 M $CuSO_4 \cdot 5H_2O$ (12 equivalents) in H_2O was added, followed by the addition of 0.1 M mono-GalNAc azide (3 equivalents) in DMSO. Finally, a 0.1 M sodium ascorbate solution (14 equivalents) in H_2O was added. The reaction mixture was stirred at 25°C at 400 rpm for 24 hours to 2 days, protected from light, and monitored by RP-HPLC.

The product was purified and its purity and identity confirmed as described in 3.4.1.

3.4.3 Preparation of tri-GalNAcB29-insulin analogue

PrgB29-insulin (1 mg, 1 equivalent) was weighed into a 1.5 mL Eppendorf, and 1 M urea in H_2O was added to prepare a 1 mM solution. To this, 0.1 M $CuSO_4 \cdot 5H_2O$ (12 equivalents) in H_2O was added, followed by the addition of 0.025 M tri-GalNAc azide (3 equivalents) in DMSO. The structure of tri-GalNAc azide is shown in Figure 9. Finally, a 0.1 M sodium ascorbate solution (14 equivalents) in H_2O was added. The reaction mixture was stirred at 25°C at 400 rpm for 24 hours to 2 days, protected from light, and monitored by RP-HPLC.

The product was purified and its purity and identity confirmed as described in 3.4.1.

3.4.4 Preparation tris-GalNAcB1-insulin

(4-ethynylbenzyl) B1-insulin (1 mg, 1 equivalent) was weighed into a 1.5 mL Eppendorf, and 1 M urea in H_2O was added to prepare a 1 mM solution. To this, 0.1 M $CuSO_4 \cdot 5H_2O$ (12 equivalents) in H_2O was added, followed by the addition of 0.025 M tris-GalNAc azide (3 equivalents) in DMSO. Finally, a 0.1 M sodium ascorbate solution (14 equivalents) in H_2O was added. The reaction mixture was stirred at 25°C at 400 rpm for 24 hours to 2 days, protected from light, and monitored by RP-HPLC The product was purified and its purity and identity conformed as described in 3.4.1.

The structures of insulin residues B1 and B29 derivatized with mono- and tri-GalNAc moieties are shown in Figure 10.

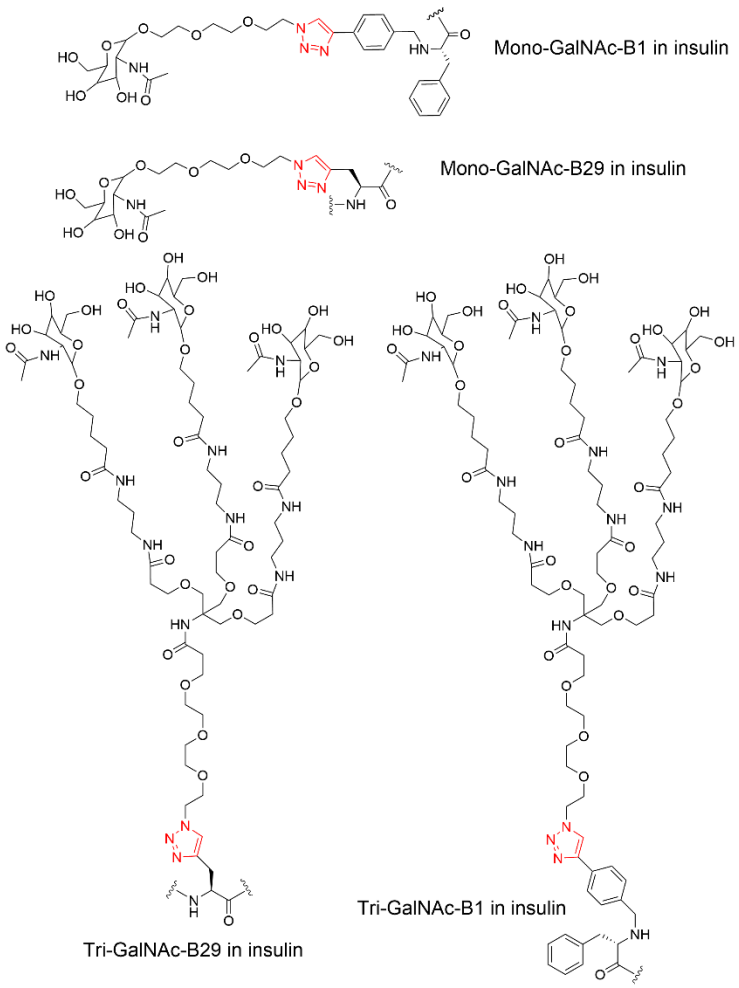

Figure 10. Structures of residues at positions B1 and B29 of insulin derivatized with mono- and tri-GalNAc moieties using click reaction. The newly formed 1,2,3-triazole bond is shown in red.

3.5 Binding affinities of glycosylated insulin analogues for human IR-A and IR-B in membranes of mouse fibroblasts

To assess binding affinities of our newly produced glycosylated insulin analogues towards both isoforms of IR, we tested the analogues in a competitive assay employing cultures of specifically transfected mouse fibroblasts. These cells have deleted mouse IGF-1 receptor [26] and are stably transfected with either human IR-A or IR-B [27]. The amount of mouse IR-A/IR-B in these cells is negligible. The principle of the assay is in a competition of a ligand for a receptor with radiolabelled human insulin.

3.5.1 Cultivation of cell cultures

Appropriate media with 10% Fetal Bovine Serum (FBS, Biosera) were pre-warmed in a 37 ºC water bath. Trypsin/EDTA solution (0.025% trypsin and 0.01% EDTA in PBS, Biosera) was warmed to room temperature (RT). All procedures were conducted under sterile conditions in a laminar flow hood. Cells were rinsed with FBS-free media and trypsinized using 34 µl/cm² of 1x trypsin/EDTA solution (Merck) for 2-5 minutes until visible detachment occurred. The cells were then collected in a 15 ml tube and centrifuged at 300 × g. After removing the supernatant, the cell pellet was resuspended in an appropriate volume of fresh media containing FBS. Cell counts were determined using either a Bürker chamber or an EVETM Automated Cell Counter (NanoEnTek). The cells were then plated at appropriate densities onto plates for further experiments or into T75 flasks for continued cultivation. All cells were incubated at 37 ºC in a 5% CO_2 humidified atmosphere. Penicillin-Streptomycin (10,000 U/ml) and L-glutamine (200 mM) were sourced from Biosera.

3.5.2 Determination of binding affinities of glycosylated insulin analogues for IR-a and IR-B

Binding affinities of analogues of insulin were determined by the competition of analogues with [^{125}I]-monoiodotyrosyl-Tyr^{A14}-human insulin for IR-A or IR-B in cell cultures. The radiolabelled insulin was prepared in IOCB as described in Asai et al. (2021) [28].

Receptor binding affinities were determined with mouse embryonic fibroblasts derived from IGF-IR knockout mice transfected with human IR-A or IR-B genes, according to Žáková et al. (2014) [29]. These cultures were maintained in DMEM with high glucose (ThermoFisher Scientific), supplemented with 10% FBS, 1% (v/v) Penicillin-Streptomycin (10,000 U/ml), 3 mg/ml puromycin and 2 mM L-glutamine and left to rest in humidified air with 5 % CO_2 at 37 ºC. The cells were seeded into 24-well plates (Schoeller; about 12 000 cells per day). The next

day the media was exchanged for FBS free media and 4-6 hours starvation period was done. FBS contains growth hormones that would interfere with the assay. After starvation period the cells were washed twice with HBB and increasing concentrations of human insulin or analogue and 43 000 cpm of ^{125}I-Tyr^{A14} human insulin (2200 Ci/mmol). The cells were then incubated and shaken for 16 h at 5 ºC. The next day after incubation period the cells were washed twice with ice cold HBB and solubilized with 0,1 M NaOH. The radioactivity was determined from the cell suspension as for IR-A or IR-B expressed cells on 2470 WIZARD^2 Automatic Gamma Counter.

The affinity binding data were analysed in GraphPad Prism 8 software. Thew individual binding curve for each analogue was determined in duplicate points, and the final dissociation constant (Kd) was calculated from at least 3 binding curves (each curve giving a single Kd value), determined independently and compared with the binding curves for human insulin. Relative binding affinities for IR-A and IR-B isoforms were calculated. The relative binding affinities is defined as (Kd of the native hormone/Kd analogue) x 100 (%).

3.6 Biological effects of tri-GalNAcB1-insulin in mice

To evaluate the ability of selected glycosylated analogue tri-GalNAc-B1-insulin to stimulate insulin signalling *in vivo*, we performed SDS-PAGE followed by Western Blotting analyses. In these analyses, the level of phosphorylation of the IR, protein kinase B (Akt) and extracellular signal-regulated kinase (Erk) was assessed.

3.6.1 Artificial induction of diabetes in mice

To study potential hepatoselectivity of our new glycosylated analogues we administered the selected analogue and human insulin *in vivo* in mice. These experiments were done by Drs. Martina Chrudinová and Lenka Žáková from Dr. Jiráček's team.

The animals were kept in the animal facility in IOCB and the experiments performed in accordance with the law of the Czech Republic Nr. 246/1992 using permission and project number 121-2023-P.

Briefly, male *C57BL/6N* mice (8 weeks old) were intraperitoneally injected with non-lethal daily doses of streptozotocin for period of 5 consecutive days to destroy physiological function of pancreatic β-cells [30]. Induction of diabetes was controlled by regular measurements of blood glucose. After 6 weeks, mice were injected to the tail vein with tri-GalNAcB1-insulin (8 units/kg, n=10) or with human insulin (2 units/kg, n=10) or with saline as a control (n=4). After injection, the animals were sacrificed by cervical dislocation and

samples of liver and epididymal white adipose tissue (eWAT) were taken one and three minutes after the injection, respectively. The samples of tissues were immediately frozen in liquid nitrogen and stored at -80 ˚C.

3.6.2 Tissue lysis

Next, tissue samples were processed to detect the activation (phosphorylation) of the proteins of interest. The lysis was performed in RIPA buffer supplemented with inhibitors of proteases and phosphatases (RIPA 1x – Merck; Cat. Numb. 20-188, 50 mM NaF, 1mM Na_3VO_4, 0.5% protease inhibitor cocktail - P8340 - SigmaAldrich). The solid tissue structure was destroyed using small metal mash balls (three per tube) put inside Eppendorf tubes (2 ml volume) each with approximately 10 mg of tissue sample and 100 µl of lysis buffer in the case of liver tissue. In case of eWAT 200 µl of buffer was used, and same amount of tissue sample was added. The tubes were put into tissue lyser (Quiagen Tissue Lyser II) where they were shaken at 30 Hz in two cycles for 1 minute. Between the cycles, the samples were cooled on ice. The lysate samples were centrifuged at 4300 rcf for 1 minute in MiniSpin® Plus (Eppendorf, Germany) to eliminate tissue debris. After centrifugation, 40 µl (for livers) or 60 µl (for eWAT tissue) of the lysate without the tissue debris was transferred into 0.5 ml Eppendorf tubes. Lysate samples were stored in -80°C until further processing.

3.6.3 Bradford assay and preparation of samples for SDS-PAGE

3.6.3.1 Bradford assay

To prepare relevant samples for Western Blotting, the concentration of proteins in the tissue lysates was determined via Bradford assay [31]. First, a calibration curve was prepared using increasing concentrations of BSA (BioSera-PM-T1725/500) in H_2O. Tissue lysates were diluted in H_2O (400x in the case of liver lysates and 200x in the case of eWAT). Subsequently, 10 µl of each sample (including blank) was mixed with the 100 µl of Bradford working solution [31] in a 96-well plate. Absorbance at 595 nm was measured on Tecan M1000 spectrometer. The concentration was determined based on the comparison of the measured absorbance of each sample with the standard curve.

3.6.3.2 Preparation of samples for SDS-PAGE

After determination of protein concentration by Bradford assay, the tissue lysates were diluted in sample buffer (1x Laemmli Sample Buffer – Bio-Rad, supplemented with 2.5% (v/v)

mercaptoethanol) to achieve 10 ug of protein in 10 µl for each sample. Then, the samples were denatured at 100° C for 1 minute and used for SDS-PAGE.

3.6.4 Testing of *in vivo* signalization of insulin and insulin derivative

3.6.4.1 Sodium dodecyl sulphate-polyacrylamide gel electrophoresis (SDS-PAGE)

The electrophoretic separation of the proteins in the tissue lysates was performed by a standard procedure in 10% polyacrylamide gel supplemented with sodium dodecyl sulphate (SDS). For protein separation, a polyacrylamide gel was prepared using equipment from Bio-Rad (USA). All solutions are shown in Tab. 2. Then, the separation gel was poured between the glass plates, 50% methanol was added to achieve a flat gel surface. Once the gel solidified, the methanol was removed, and the gel's upper surface was dried using filter paper. Finally, the stacking gel solution (as specified in Table 2) was applied, and a plastic 15-well comb was inserted into the gel to create wells.

Table 2 Chemicals and composition of gels used in SDS-PAGE

	Separation gel (10 %)	Stacking gel (4 %)
MilliQ® water	3 ml	2.7 ml
30 % acrylamide mix	2.5 ml	670 µl
Tris/HCl	1.9 ml (pH 8.8)	500 µl (pH 6.8)
10 % SDS (v/v)	75 µl	40 µl
10 % APS (w/v)	75 µl	40 µl
TEMED	3 µl	4 µl

The gels were then placed into the electrophoretic apparatus (Bio-Rad, USA) and filled to the designated mark with electrophoretic buffer (25 mM Tris, 192 mM glycine, 0.01% SDS (w/v)). The comb was removed, and the samples (10 µg of protein in 10 µl sample buffer for each sample) were loaded. For molecular weight markers, 3 µl of Precision Plus Protein™ Dual Color Standard were used. The apparatus was connected to a power supply (Bio-Rad, USA). Protein separation was performed under the following conditions: the initial current was limited to 12 mA per gel, with a starting voltage of 100 V for 10 minutes, followed by an increase in current to 24 mA per gel and voltage to 200 V for approximately 1 hour.

3.6.4.4 Western blotting

After the electrophoresis was finished, we took the gels out of plates and the gels were put into transfer buffer (20 mM Tris, 189 mM glycine, 10% methanol (v/v), 0.1% SDS (w/v)) for 30

minutes and the Western blotting followed. Western blotting was done in the apparatus for semi-dry western blotting from BioRad. The PVDF membrane (Immobilion ®-P transfer membrane) and 2 pieces of thick filtration paper were cut to have size of 8.8 x 6 cm. The PVDF membrane was activated in methanol, washed in MIlliQ H_2O and incubated in transfer buffer for 15 minutes. The filtration papers were also soaked in transfer buffer at room temperature for approximately 1 min. The PVDF membrane was placed onto one filtration paper in blotting apparatus and air bubbles were rolled out. The gels were put onto PVDF membrane and topped with second filtration paper. The air bubbles were rolled out again. The voltage was set to 12 V and current to 1.5 mA/cm^2 for 1.5 hour. The PVDF membrane was incubated for 1 hour in 20 ml of 5% (w/v) solution of BSA (BioSera-PM-T1725/500) in T-TBS (20mM Tris/HCl, 140 mM NaCl, 0,1 % Tween-20 (v/v)) at room temperature. After that the membrane was cut to three pieces according to the molecular weight markers (at 75 and 50kDa). The membrane stripes were then put in solutions of appropriate primary antibodies. The stripe with proteins bigger that 75 kDa was submerged into antibody for phosphorylated β-subunit of insulin/IGF-1 receptor (95 kDa), the stripe with proteins of 75-50 kDa was submerged into antibody solution for phosphorylated Akt (phosphorylated protein kinase B, 60 kDa), and the stripe with proteins below 50kDa was submerged into antibody solution for phosphorylated Erk (extracellular signal-regulated kinase, 44 and 42 kDa). The antibodies were diluted in 5% (w/v) BSA in T-TBS and the details of used antibodies and their specific dilutions are shown in Table.1 (3.1.1). Membranes were incubated in antibody solutions overnight at 4° C.

After overnight incubation with the primary antibodies, the membranes were washed 3 times for 5 minutes in T-TBS buffer and then incubated in solution of secondary antibodies (details on antibodies are provided in Table 1). In the case of all primary antibodies for phosphorylated proteins, rabbit secondary antibody conjugated with horseradish peroxidase was used. The secondary antibody was diluted In 5% dried milk in T-TBS. The membranes were incubated for 1 hour at room temperature. After that, the membranes were washed 3-times with T-TBS buffer for 5 minutes and once for 10 minutes at the end. For signal detection, SuperSignal™ West Femto Maximum Sensitivity Substrate (Thermofisher) was used and the phosphorylated proteins of interest were visualized using ChemiDoc MP Imaging System (Bio-Rad). After detection of the phosphorylated proteins, total GAPDH was detected for signal normalization. To this end, the membranes containing proteins below 50kDa were re-incubated in antibody for GAPDH (36 kDa, details provided in Table 1). The procedure was same as

described above, except of using anti-mouse secondary antibody (1:20000 in 5 % (w/v) in dried milk in T-TBS) (see Table 1).

After analysis of data with ImageLab software, signal of each phosphorylated protein was normalized to the GAPDH signal from the respective sample. Five technical replicates were obtained for each sample. The intensities of signals from each western blot were related towards average value of HI signals in given set of experiment. The results were statistically evaluated in GraphPad Prism 8 using Ordinary One Way ANOVA.

4. Results

4.1 Synthesis of precursor octapeptide for the semisynthesis of PrgB29-insulin

After HPLC purification of Gly-Phe-Phe-Tyr-Thr-Pro-Prg-Thr peptide (Prg is L-propargylglycine, Figure 8) we obtained about 62 mg of the product (about 67 μmol, 67 % yield). The chromatogram of HPLC purification of the peptide is shown in Figure 11 and Figure 12 shows mass spectrometry analysis of the product.

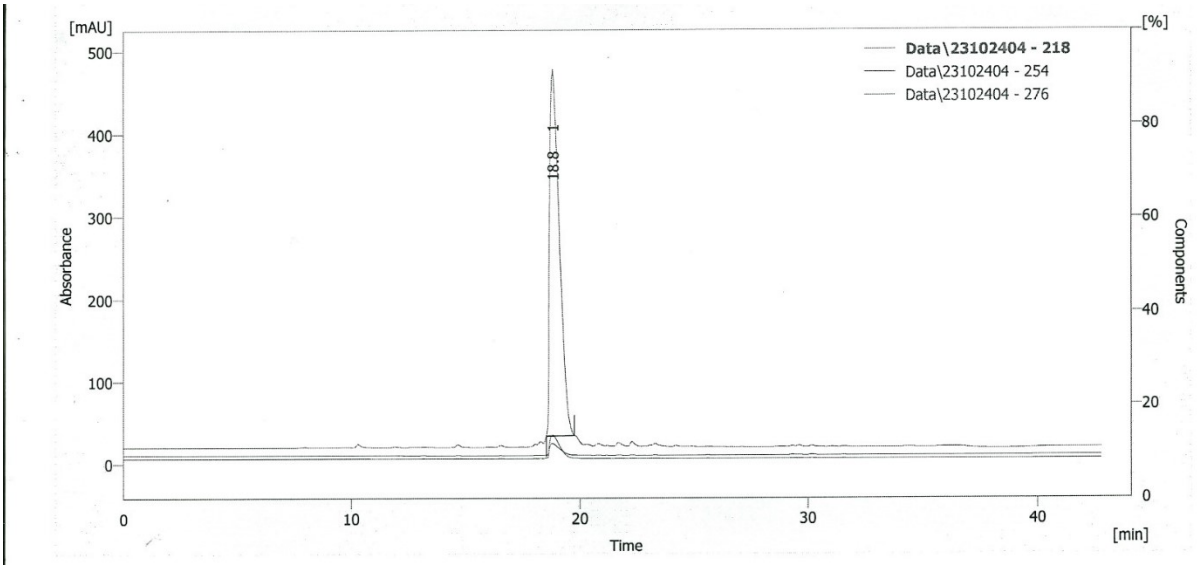

Figure 11. HPLC purification of Gly-Phe-Phe-Tyr-Thr-Pro-Prg-Thr peptide. Details are in Methods.

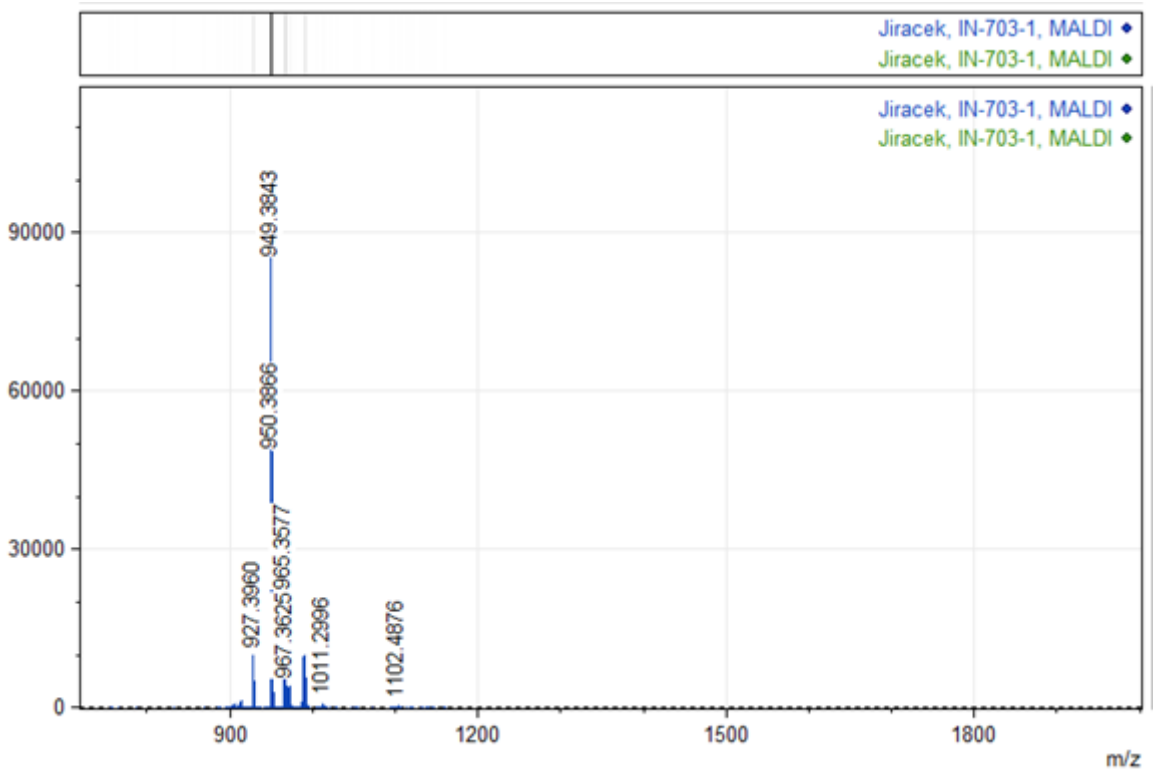

Figure 12. Low resolution MALDI mass spectrum of GFFYTP(Prg)T peptide ($C_{47}H_{58}N_8O_{12}$, Exact Mass: 926.4174, Molecular Weight: 927.0250). The m/z signal 949.38 represents the target molecule with sodium atom aduct.

4.2 Enzymatic semisynthesis of PrgB29-insulin

The semisynthetic reaction of des(B23-B30)-insulin (DOI) with GFFYTP(Prg)T octapeptide gave 3.1 mg (0.54 μmol) of the product (PrgB29-insulin). The limiting component of this trypsin-catalysed reaction was DOI (3.08 μmol was used) and, therefore, the product was prepared in 17.5 % yield. Analytical HPLC chromatogram of the product and ESI HR mass spectrum are shown in Figures 13 and 14, respectively.

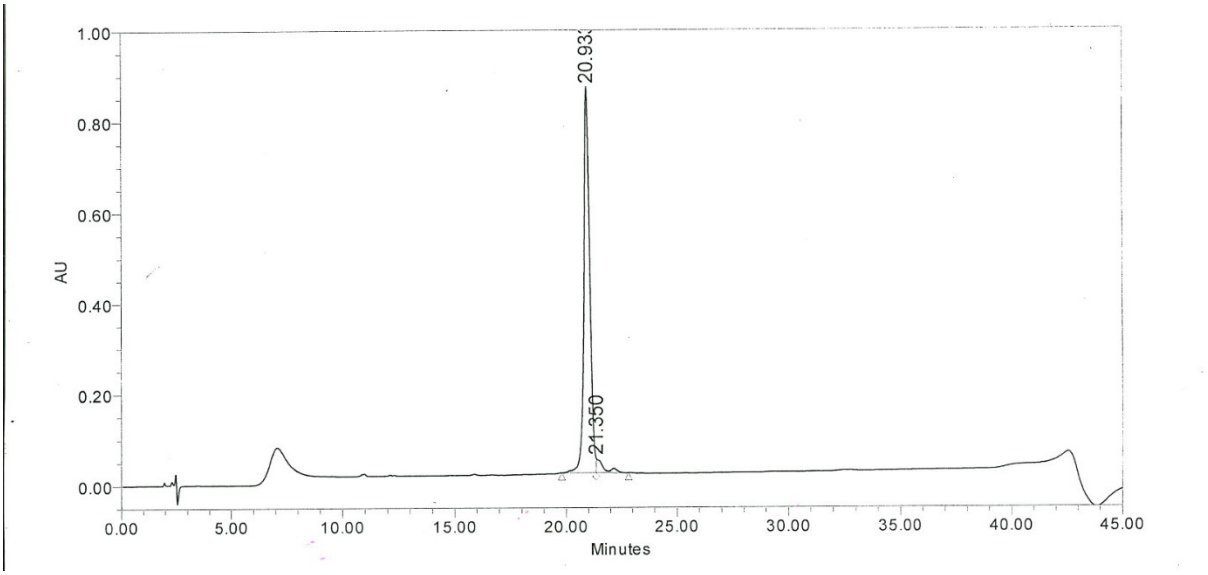

Figure 13. Analytical HPLC chromatogram of PrgB29-insulin. Details are in Methods.

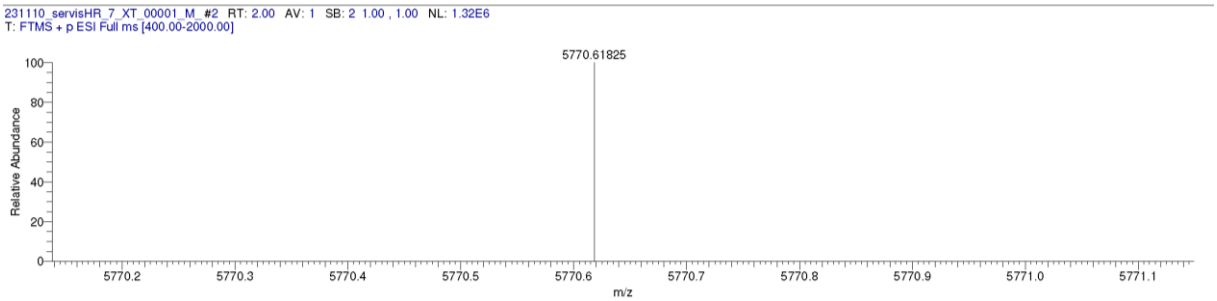

Figure 14. High resolution ESI mass spectrum of PrgB29-insulin ($C_{256}H_{376}N_64O_{77}S_6$, Exact Mass: 5770.5798, Molecular Weight: 5774.5550. The deconvoluted m/z signal 5770.6182 represents exact mass of the product.

4.3 Preparation of (4-ethynylbenzyl) B1-insulin

The reaction of 40 mg (6.89 μmol) of zinc-free human insulin with 4-ethynylbenzaldehyde/$NaBH_3CN$ gave 7.8 mg of HPLC pure product. This represents about 19 % yield. Analytical chromatogram of the product is shown in Figure 15 and the mass spectroscopy spectrum is shown in Figure 16.

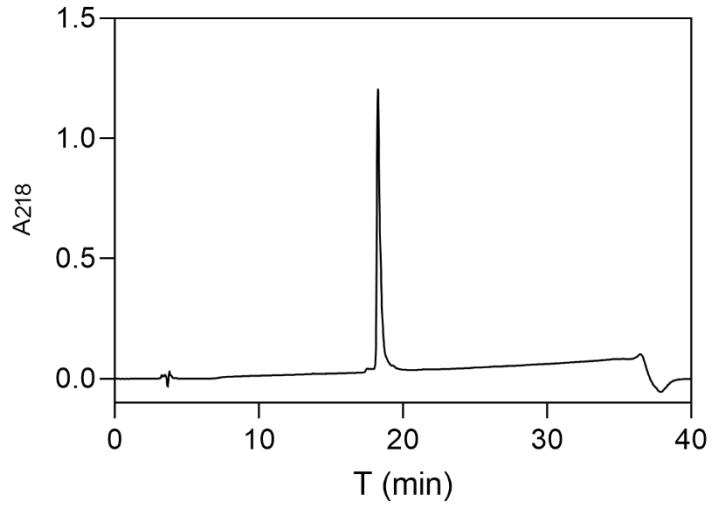

Figure 15. Analytical HPLC chromatogram of (4-ethynylbenzyl) B1-insulin. Details are in Methods.

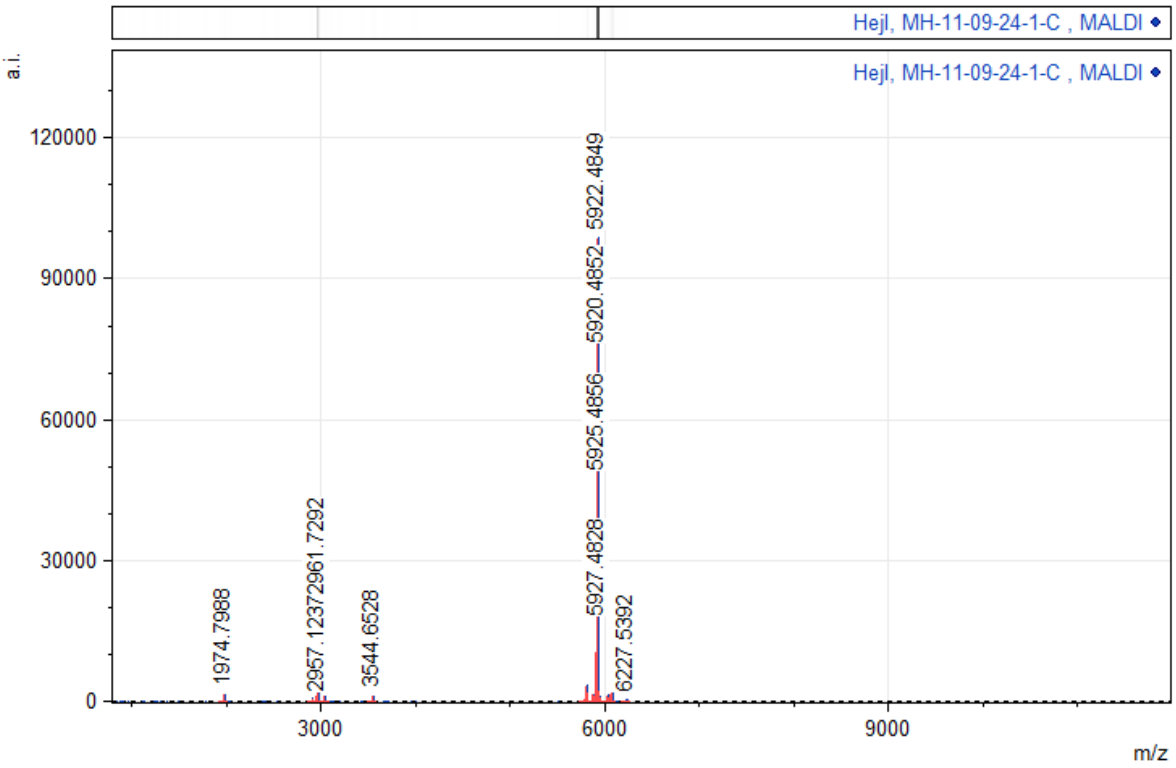

Figure 16. Low resolution MALDI mass spectrum of (4-ethynylbenzyl) B1-insulin ($C_{266}H_{389}N_{65}O_{77}S_6$, Exact Mass: 5917.6846, Molecular Weight: 5921.7760).

4.4 Preparation of B29- and B1-glycosylated insulins

4.4.1 Preparation of mono-GalNAcB29-insulin

The click reaction of PrgB29-insulin (1 mg, 0.170 µmol) with mono-GalNAc azide was performed several times and the typical yield was about 0.15 mg (0.024 µmol) of mono-

GalNAcB29-insulin, which is about 14 %. Analytical chromatogram of the product is shown in Figure 17 and the mass spectroscopy spectrum is shown in Figure 18.

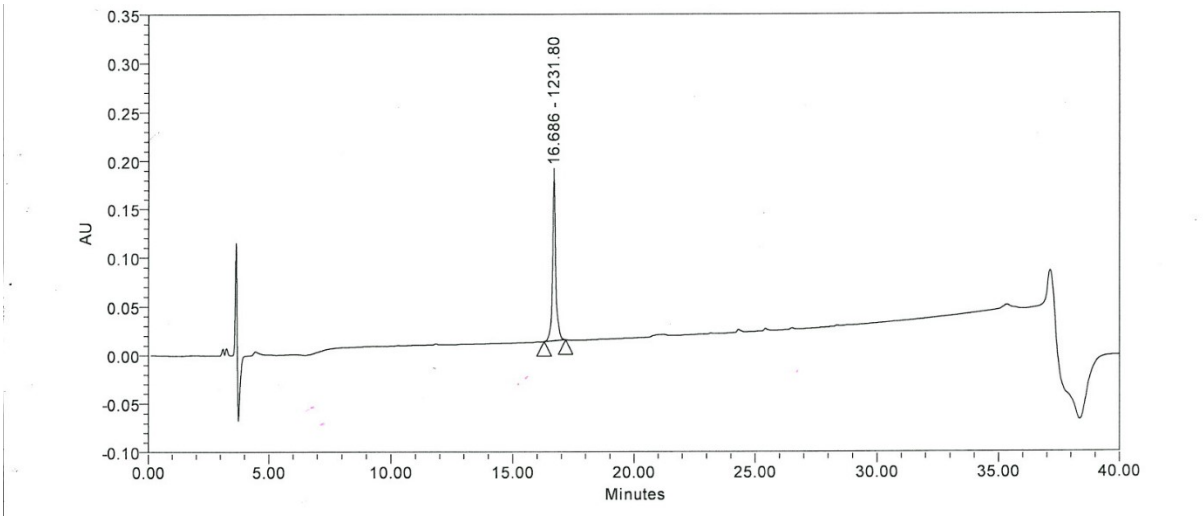

Figure 17. Analytical HPLC chromatogram of mono-GalNAcB29-insulin. Details are in Methods.

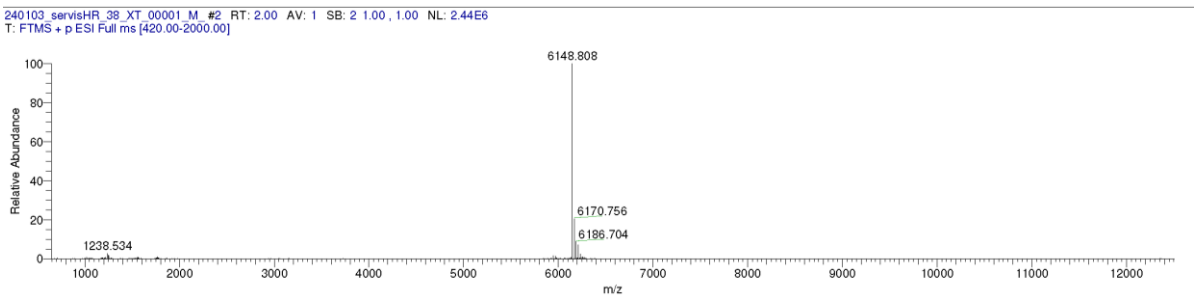

Figure 18. Deconvoluted high resolution ESI mass spectrum of mono-GalNAcB29-insulin ($C_{270}H_{402}N_{68}O_{85}S_6$, Exact Mass: 6148.808, Molecular Weight: 6152.9370).

4.4.2 Preparation of mono-GalNAcB1-insulin

The click reaction of (4-ethynylbenzyl) B1-insulin (1 mg, 0.170 µmol) with mono-GalNAc azide was performed several times and the typical yield was about 0.17 mg (0.027 µmol) of mono-GalNAcB29-insulin, which is about 16 %. Analytical chromatogram of the product is shown in Figure 19 and the mass spectroscopy spectrum is shown in Figure 20.

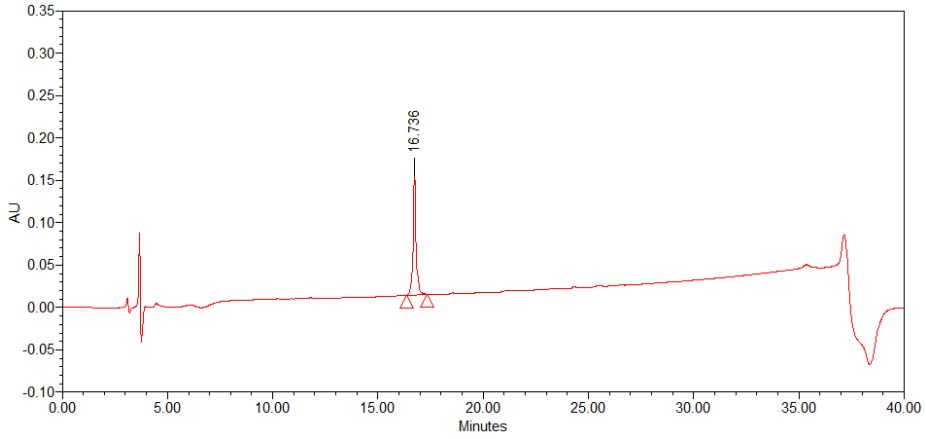

Figure 19. Analytical HPLC chromatogram of mono-GalNAcB1-insulin. Details are in Methods.

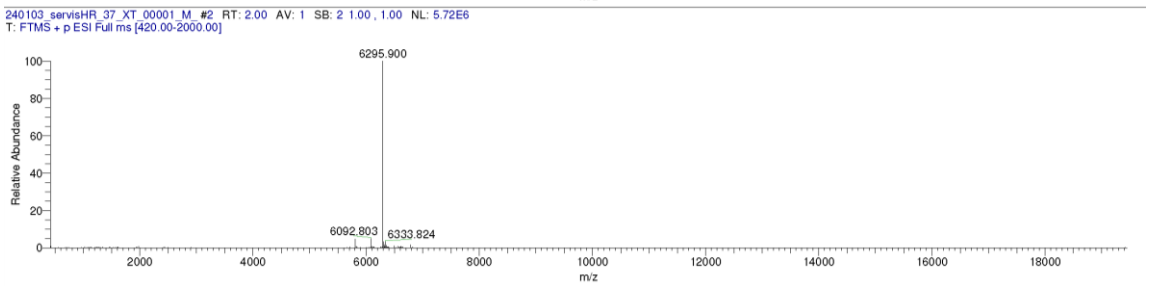

Figure 20. Deconvoluted high resolution ESI mass spectrum of mono-GalNAcB1-insulin ($C_{280}H_{415}N_{69}O_{85}S_6$, Exact Mass: 6295.900, Molecular Weight: 6300.1580).

4.3.3 Preparation of tri-GalNAcB29-insulin

The click reaction of PrgB29-insulin (1 mg, 0.170 µmol) with tri-GalNAc azide was performed several times and the typical yield was about 0.11 mg (0.015 µmol) of tri-GalNAcB29-insulin, which is about 8.7 %. Analytical chromatogram of the product is shown in Figure 21 and the mass spectroscopy spectrum is shown in Figure 22.

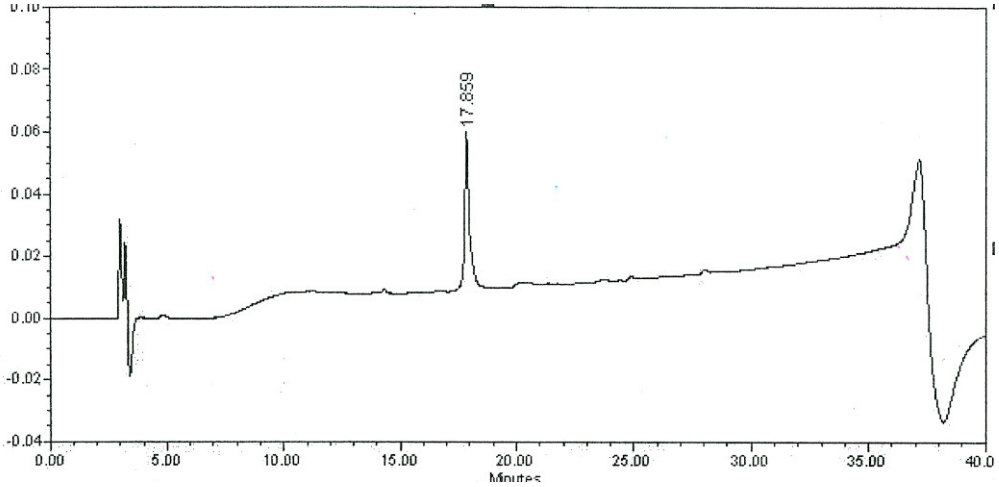

Figure 21. Analytical HPLC chromatogram of tri-GalNAcB29-insulin. Details are in Methods.

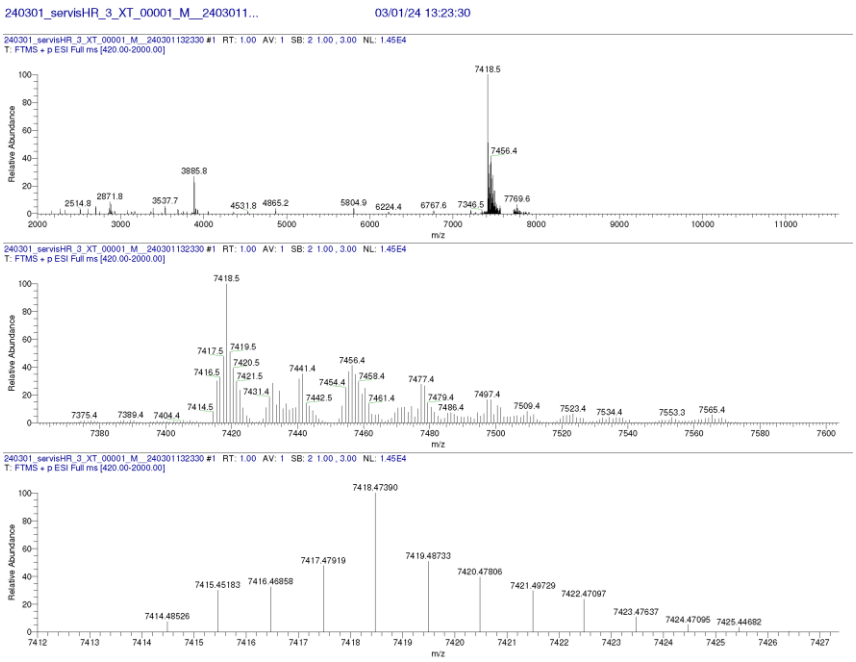

Figure 22. Deconvoluted high resolution ESI mass spectrum of tri-GalNAcB29-insulin ($C_{326}H_{501}N_{77}O_{108}S_6$, Exact Mass: 7414.4402, Molecular Weight: 7419.3850).

4.3.4 Preparation of tri-GalNAcB1-insulin

The click reaction of PrgB29-insulin (1 mg, 0.170 µmol) with tri-GalNAc azide was performed several times and the typical yield was about 0.13 mg (0.17 µmol) of tri-GalNAcB1-insulin, which is about 10 %. Analytical chromatogram of the product is shown in Figure 23 and the mass spectroscopy spectrum is shown in Figure 24.

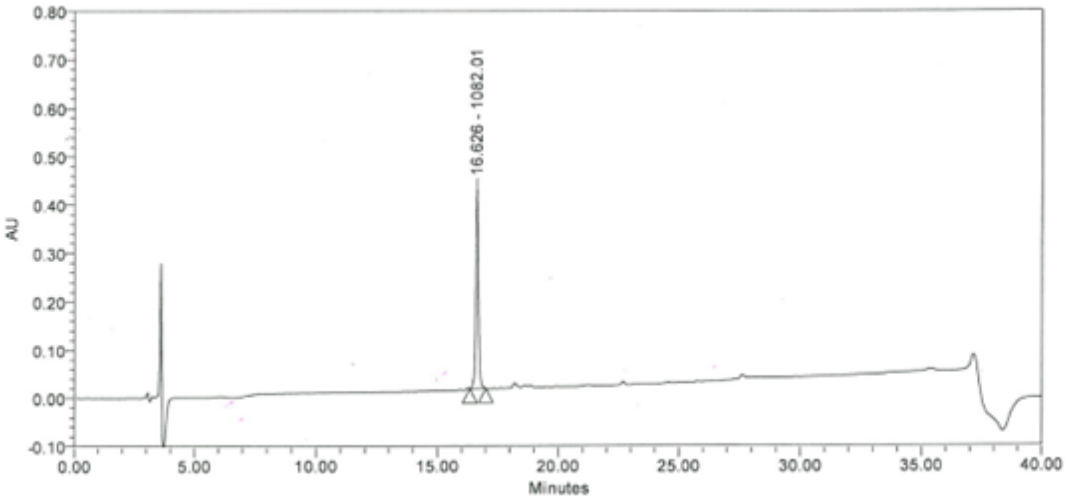

Figure 23. Analytical HPLC chromatogram of tri-GalNAcB1-insulin. Details are in Methods.

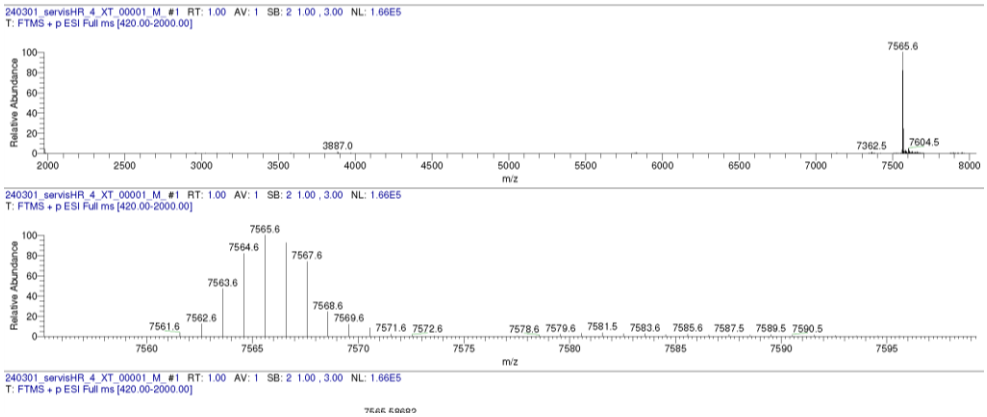

Figure 24. Deconvoluted high resolution ESI mass spectrum of tri-GalNAcB1-insulin ($C_{336}H_{514}N_{78}O_{108}S_6$, Exact Mass: 7561.5450, Molecular Weight: 7566.6060).

4.4 Binding affinities of glycosylated insulin analogues for human IR-A and IR-B in membranes of mouse fibroblasts

The binding affinities of mono-GalNAcB1-insulin, mono-GalNAcB29-insulin, tri-GalNAcB1-insulin and tri-GalNAcB29-insulin for human IR-A and IR-B are shown in Tables 1-4. Mono-GalNAc and tri-GalNac insulins were measured with IR-A or IR-B in separated series of experiments and for each series of measurements, the binding affinity of human insulin was determined in parallel. Representative binding curves of the analogues and human insulin on IR-A are shown in Figure 25 and on IR-B in Figure 26.

Table 3. Binding affinities of mono-GalNAc insulin analogues for IR-A. The relative binding affinities is defined as (Kd of the native hormone/Kd analogue) x 100 (%).

Analogue	Kd ± S.D. (nM), n = 3	Relative binding affinity (in %)
Human insulin	0.29 ± 0.07	100
mono-GalNAcB1-insulin	0.82 ± 0.13	35
mono-GalNAcB29-insulin	0.76 ± 0.30	38

.

Table 4. Binding affinities of mono-GalNAc insulin analogues for IR-B. The relative binding affinities is defined as (Kd of the native hormone/Kd analogue) x 100 (%).

Analogue	Kd ± S.D. (nM), n = 3	Relative binding affinity (in %)
Human insulin	0.42 ± 0.02	100
mono-GalNAcB1-insulin	1.21 ± 0.30	35
mono-GalNAcB29-insulin	1.51 ± 0.29	28

Table 5. Binding affinities of tri-GalNAc insulin analogues for IR-A. The relative binding affinities is defined as (Kd of the native hormone/Kd analogue) x 100 (%).

Analogue	Kd ± S.D. (nM), n = 3	Relative binding affinity (in %)
Human insulin	0.23 ± 0.04	100
tri-GalNAcB1-insulin	2.0 ± 0.76	11.5
tri-GalNAcB29-insulin	9.2 ± 5.0	2.5

Table 6. Binding affinities of tri-GalNAc insulin analogues for IR-B. The relative binding affinities is defined as (Kd of the native hormone/Kd analogue) x 100 (%).

Analogue	Kd ± S.D. (nM), n = 3	Relative binding affinity (in %)
Human insulin	0.45 ± 0.05	100
tri-GalNAcB1-insulin	1.7 ± 0.6	26
tri-GalNAcB29-insulin	5.9 ± 1.3	7.6

The binding affinities of the mono-GalNac insulins were similar for the B1 and B29 derivatives, as well as for IR-A and IR-B, all reaching approximately 30% of human insulin (28-38%).

The tri-GalNac insulins were generally less potent than mono-GalNac insulins, especially on IR-A and B29-modified derivative was less potent than its B1 counterpart. Tri-GalNacB1-insulin still retained a reasonable binding affinity for IR-B (26% of human insulin) and due to its lower affinity for IR-A (11.5% of human insulin), this analogue also displayed some IR-B binding specificity, being about 2.3-times more specific for IR-B (26/11.5). Still reasonable binding affinity of tri-GalNacB1-insulin for IR-B, its enhanced specificity of binding for IR-B and the fact that glycosylated ligands with three GalNAc groups are considered as the best binders for ASGP receptor [24] led us to conclusion that tri-GalNac-B1-insulin is the best candidate for further *in vivo* experiments in mice.

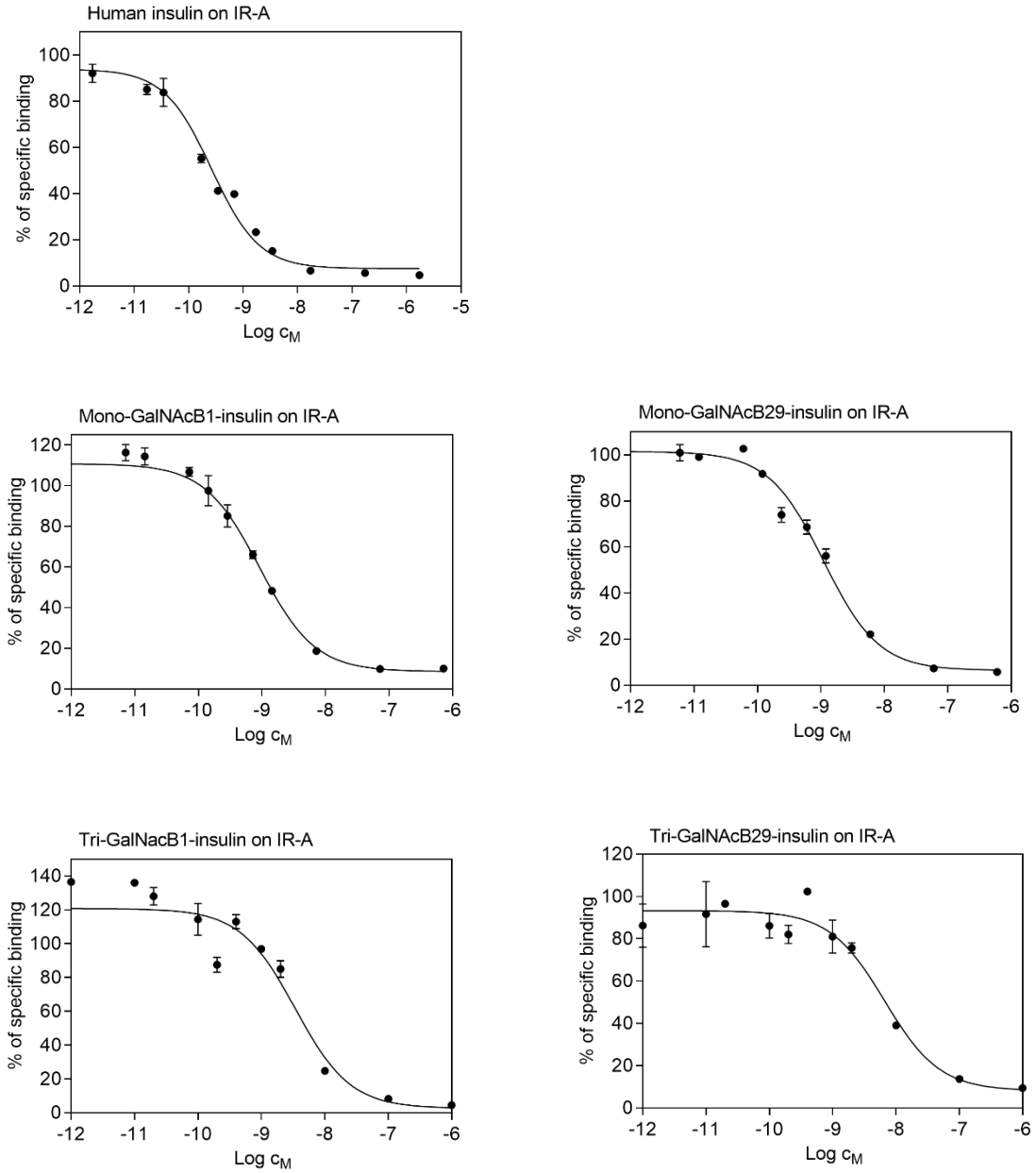

Figure 25. Representative binding curves of human insulin and glycosylated insulin derivatives on IR-A.

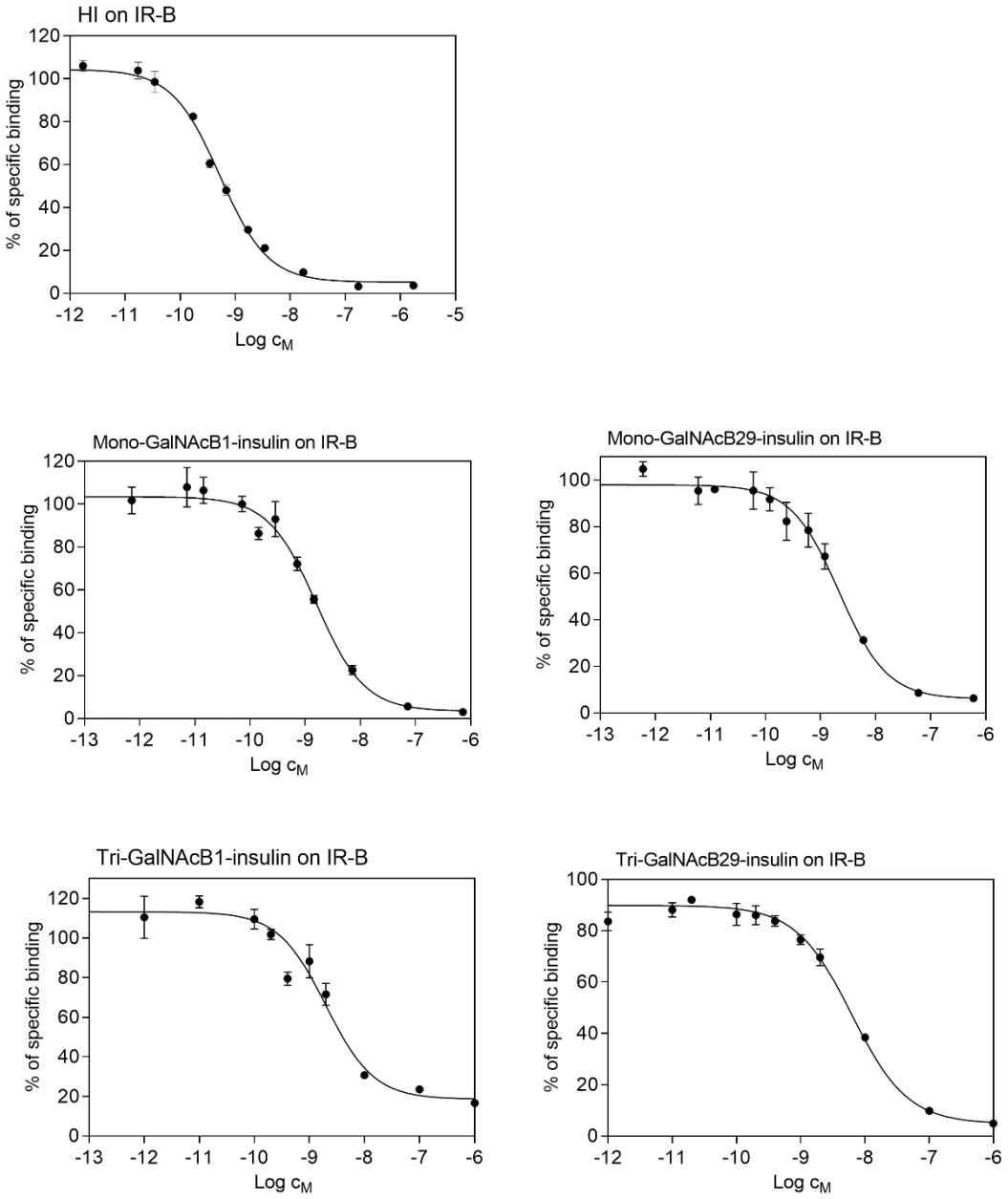

Figure 26. Representative binding curves of human insulin and glycosylated insulin derivatives on IR-B.

4.5 In vivo tests of tri-GalNAcB1-insulin in mice

The mice subjects were treated as described in chapter 3.6.1 and the samples of our target tissues prepared (liver tissue and eWAT) as described in chapter 3.6.2 and 3.6.3. Then, the SDS-PAGE with Western-blot assay followed as described in chapter 3.6.4. The electrophoreses and Western-blots were conducted five times for each sample to gain a proper statistical sample. The final data were analysed, processed and evaluated in BIORAD ImageLab and final graphs prepared in GraphPad Prism 8.0. The electrophoretic analyses of liver tissues (shown in Figure

27) were primarily conducted by Dr. Martina Chrudinová from J. Jiráček's laboratory, with my partial contribution, while the electrophoretic analyses of eWAT samples (shown in Figure 28) were performed by myself. Statistical evaluation of Western-blot results was done by Dr. M. Chrudinová. The western blots used for the analysis of liver samples are shown in Figure 27 and the western blots obtain for eWAT samples are shown in Figure 28. Results from mouse liver samples are shown in Figure 29. Each point represents an average value obtained from five independent electrophoretic/Western-blot experiments.

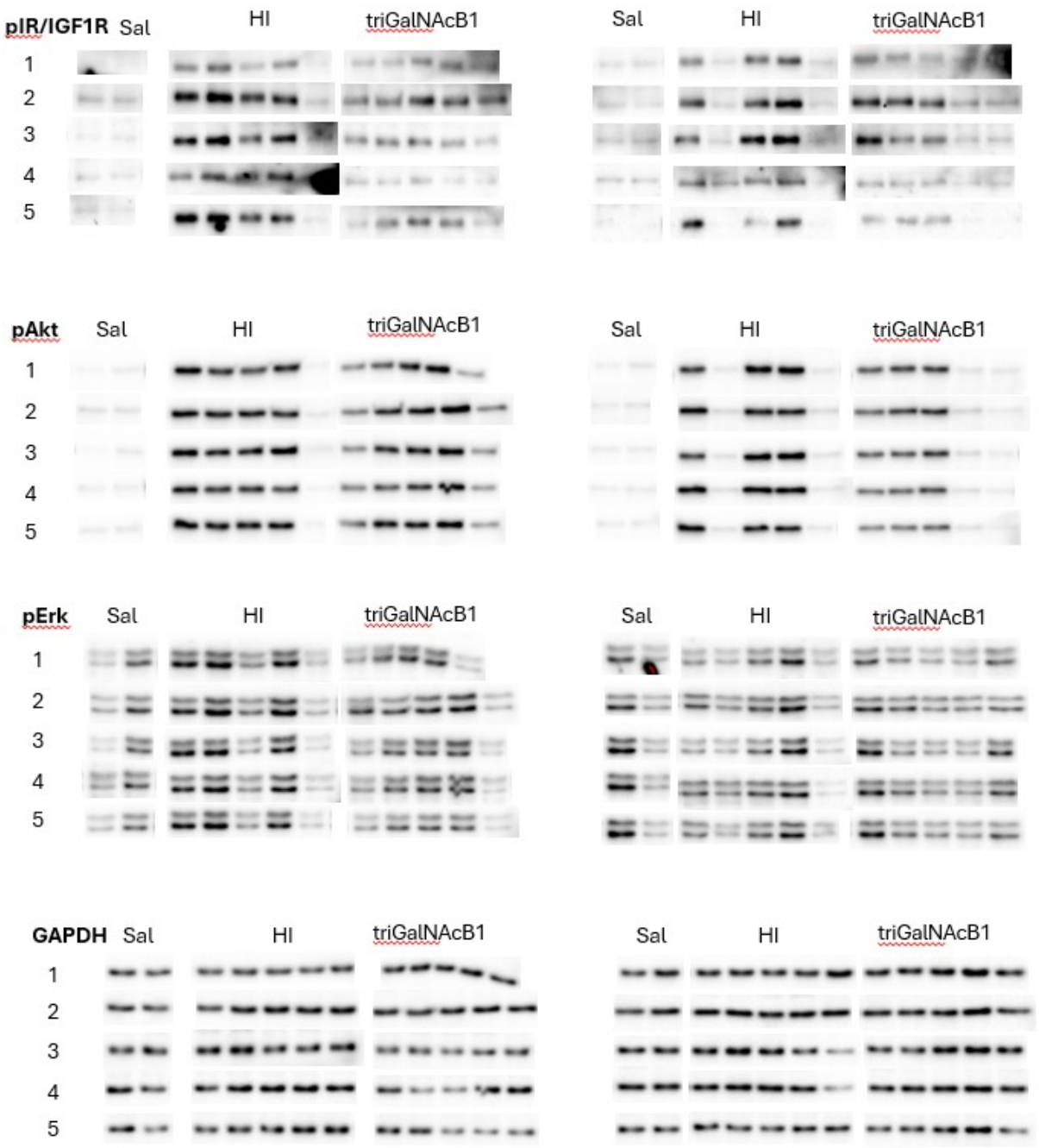

Figure 27. Western-blot analyses of samples from liver tissues from mice stimulated with saline (four animals), human insulin (HI, ten animals) and triGalNacB1-insulin (ten animals). Each electrophoretic experiment was repeated five times (lines 1-5), each time on two separate gels. Proteins detected in assays were phosphorylated insulin/IGF-1 receptor tyrosine kinase (pIR/IGF1R), phosphorylated protein kinase B (pAkt) and phosphorylated extracellular signal-regulated kinase (pErk). Analysis of the GAPDH protein was used as a control for proper protein loading, and the data were normalized to the density value of the GAPDH protein in the respective experiments.

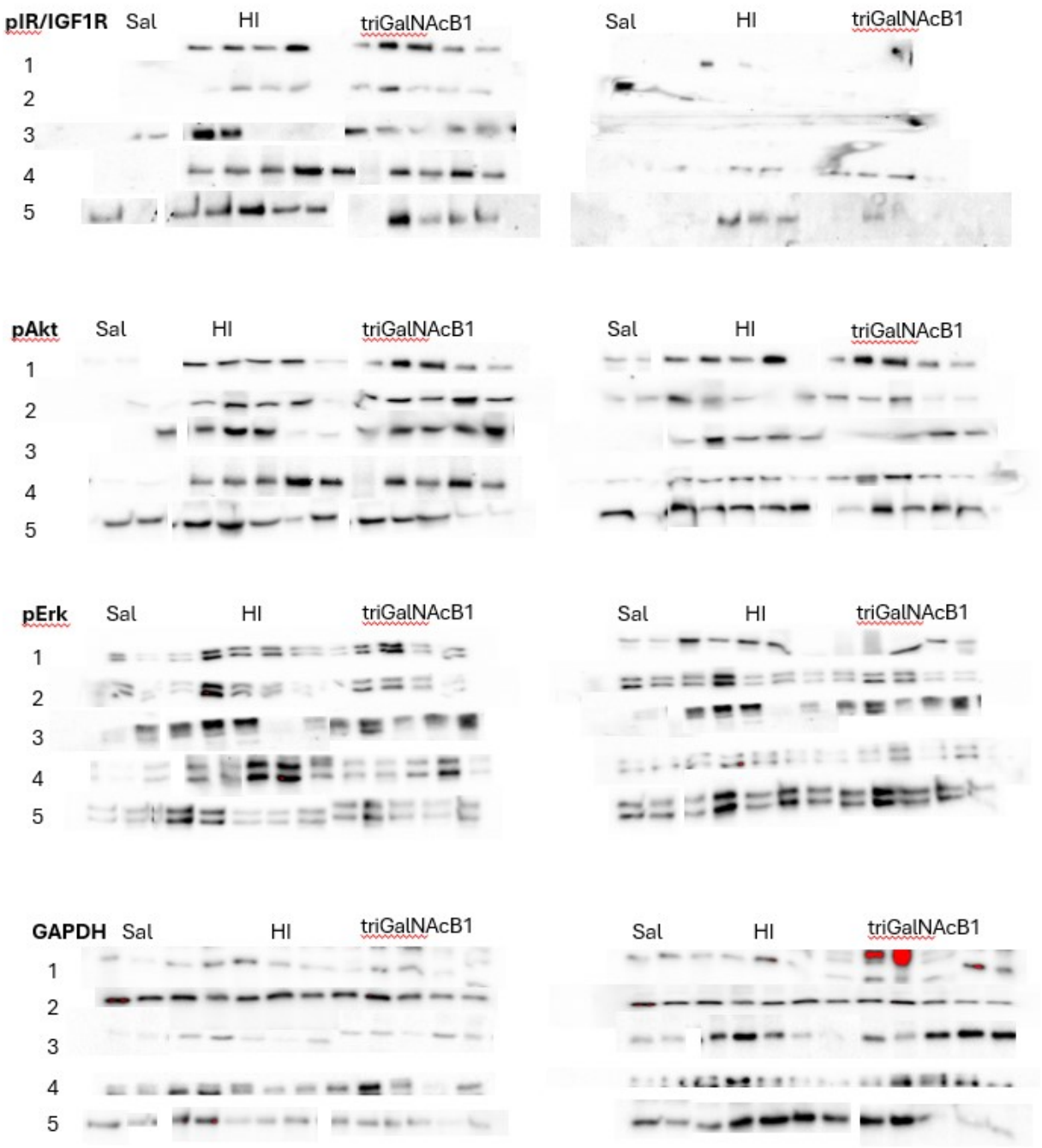

Figure 28. Western-blot analyses of samples from eWat tissues from mice stimulated with saline (four animals), human insulin (HI, ten animals) and triGalNacB1-insulin (ten animals). Each electrophoretic experiment was repeated five times (lines 1-5), each time on two separate gels. Proteins detected in assays were phosphorylated insulin/IGF-1 receptor tyrosine kinase (pIR/IGF1R), phosphorylated protein kinase B (pAkt) and phosphorylated extracellular signal-regulated kinase (pErk). Analysis of the GAPDH protein was used as a control for proper protein loading, and the data were normalized to the density value of the GAPDH protein in the respective experiments.

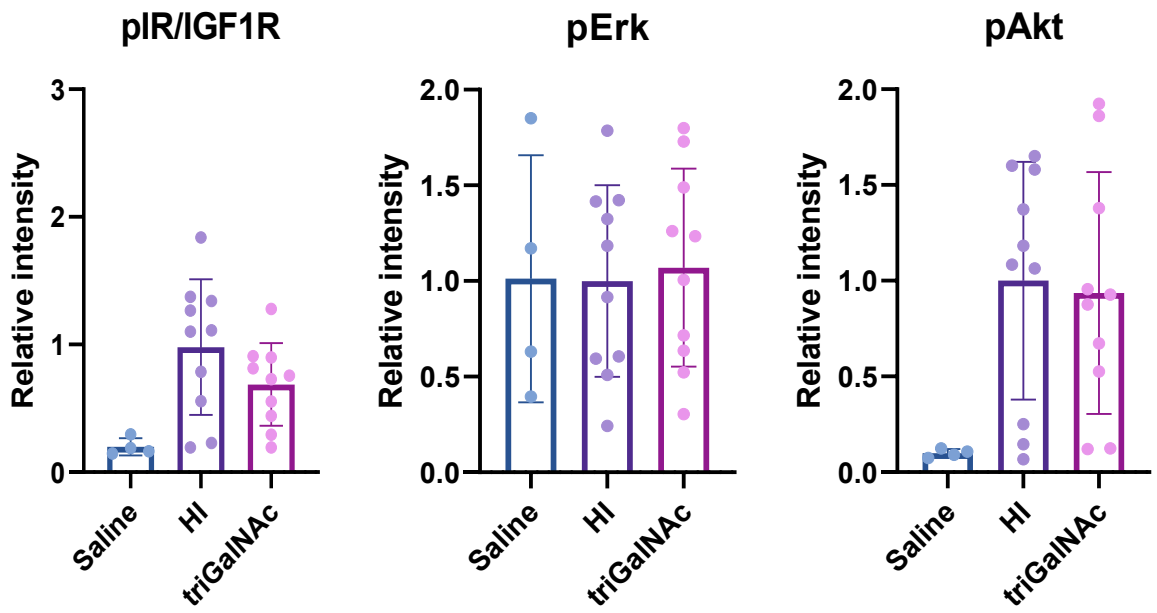

Figure 29. Results from electrophoretic/Western-blot analyses of samples from mouse liver tissues treated with saline (four animals), human insulin (HI, ten animals) and tri-GalNAcB1-insulin (IN-ML-84, ten animals). Each point represents an average value obtained from one animal in five independent electrophoretic experiments. An asterisk shows that there is a statistically significant difference between results with saline and human insulin ($P < 0.05$).

The data in Figure 29 show that tri-GalNAcB1-insulin does not elicit differential activation of the insulin receptor (and IGF receptor, but it's not highly presented on liver tissue), Akt, and Erk phosphorylation in the liver compared to human insulin. While there is a trend suggesting weaker activity of tri-GalNAcB1-insulin in IR activation, the difference between insulin and the analogue is not statistically significant. Moreover, despite a strong trend, we have not observed statistically significant difference between effects of saline and of tri-GalNAcB1-insulin in stimulation of IR phosphorylation. On the other hand, human insulin stimulated statistically stronger effects on activation of IR and Akt in liver. Phosphorylation of Erk was not affected neither by insulin or by tri-GalNAcB1-insulin analogue.

We did not statistically evaluate the results of Western blot analyses of samples from eWAT tissue shown in Figure 28. The quality of the primary data was low and did not allow for obtaining any relevant information through statistical analysis (data not shown).

5 Discussion

In this study, we examined in vitro properties in cells and biological effects in animals of newly developed glycosylated insulin analogues. These innovative compounds are formed by linking human insulin to GalNAc-based moieties. Conjugates of GalNac moieties with siRNAs have been shown in previous research to serve as targeting molecules for hepatocytes through binding to liver hepatocyte ASGPR receptor [24]. Preferential hepatic targeting of insulin in vivo has the potential to enhance the effectiveness of insulin doses in diabetic patients, leading to increased hepatic action and more physiological profiles of glycaemia.

For the covalent attachment of GalNAc group to insulin we used a specific reaction that belongs to a family of reactions that are called a “click chemistry”. The term "click chemistry" wand K. B. Sharpless in 2001 [32] to describe reactions that are efficient, broadly applicable, and produce minimal byproducts, which can be easily removed. These reactions are stereospecific, simple to execute, and can be carried out in benign or easily removable solvents. The concept emerged alongside growing interest in the pharmaceutical, materials, and other industries for methods that enable the rapid generation of large compound libraries for screening in discovery research We utilized the copper(I)-catalyzed azide–alkyne 1,3-cycloaddition (CuAAC) [33], a prototypical click reaction that increases reaction rates by 10^7 to 10^8-fold relative to the uncatalyzed 1,3-dipolar cycloaddition. It performs well across a wide temperature range, is compatible with aqueous conditions and pH levels from 4 to 12 and tolerates a variety of functional groups. Pure products can be easily isolated through simple filtration or extraction, without requiring chromatography or recrystallization. The active Cu(I) catalyst can be generated either from Cu(I) salts or by reducing Cu(II) salts using sodium ascorbate (Figure 29).

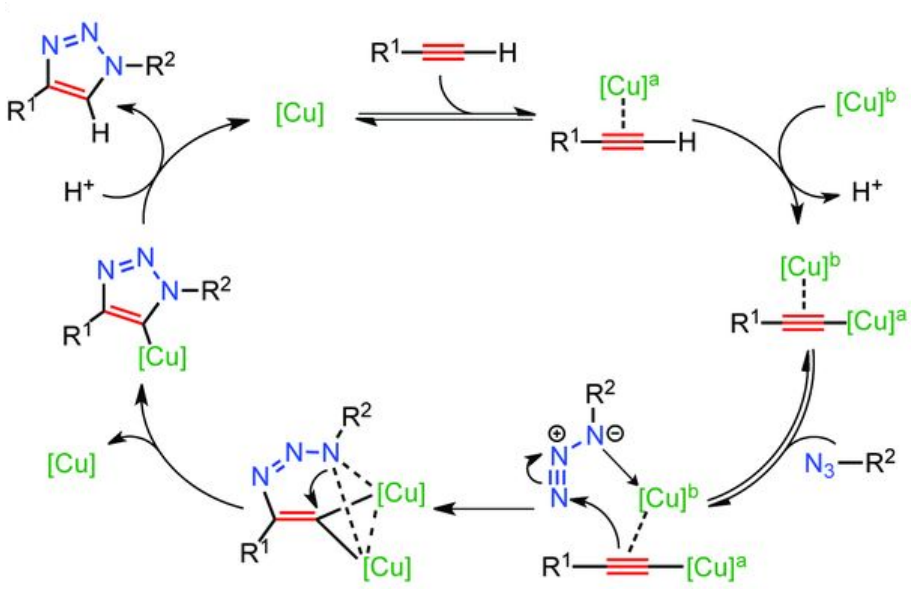

Figure 29. Molecular mechanism of copper(I)-catalyzed azide-alkyne 1,3-cycloaddition [32]

Two forms GaNAc derivates were used in our experiments (Figure 9). These forms have either one or three N-acetylgalactosamine groups attached to a polyethylene glycol linker with an azido group. Mono-GalNAc construct is shorter and tri-GalNac is longer and its galactosamine moieties are attached in a form of dendrimer. The available literature clearly shows that the three GalNAc groups are the preferred form of a ligand for ASGPR receptor [24]. The reason for which we probed both forms, mono- and tri-GalNAc, was to test the efficiency of the click reactions with alkyne derivatives of insulin. Mono-GalNAc azide was used the first because tri-GalNAc azide is more expensive and also bulkier reactant.

For click reactions, it was also necessary to prepare derivative(s) of insulin with terminal alkyne group. Two positions in insulin are usually considered to be accessible for modifications without too negatively affect bioactivity of the hormone. It is first LysB29 which is often used for modifications of insulin with lipids or polyethylene glycol moieties [34]. Second, the PheB1 of insulin can be selectively modified due it lower pK_a of its primary amino group [35]. In our study, we used both these positions. Alkyne group to B29 was introduced by synthesis of B-chain C-terminal octapeptide of insulin where L-propargylglycine used was instead of Lysine at B29. This octapeptide was attached to des(B23-B30)insulin (DOI) by semisynthesis with a reasonable of yield that of PrgB29-insulin further chemistry with GalNAc moieties. In parallel, the amino group at the position B1 of insulin was reacted at pH 5.5-60 with ethynyl benzaldehyde and the resulting Schiff's base reduced with sodium cyanoborohydride also in a good yield that also allowed further chemistry with the (4-ethynylbenzyl) B1-insulin product.

The remarkable advantage of this reaction is its selectivity in the presence of A1 and B29 amino groups [36].

Both alkyne insulins were used for CuAAC reactions with mono- and tri-GalNac azides. The yields of reactions with mono-GalNac azides were similar for both alkyne insulins (14-16%). The yields for tri-GalNac azides were significantly lower but also similar for B1 and B29 alkyne insulins (9-10%). These results clearly demonstrate that bulkier moiety of tri-GalNac azide is less efficient in the click reactions with insulin.

The binding assays with new glycosylated insulins were conducted on genetically modified fibroblasts overexpressing IR-A or IR-B. B1 and B29 Mono-GalNAc insulins behave similarly on both isoforms and do not display and isoform selectivity (all between 28-38% of binding affinity of human insulin). Tri-GalNAc insulins were much less active (probably due to higher bulkiness of tri-GalNac group), especially B29-derivative but, on the other hand, they showed some moderate selectivity for IR-B (Tables 3 and 4). Especially, tri-GalNacB1-insulin still retained reasonable binding for IR-B (26% of human insulin) and its affinity for IR-A was about 11% of human insulin.

For further biological evaluation, we selected tri-GalNacB1-insulin, because its moderate IR-B specificity can add some benefit to its potential hepatoselective action caused by B1-glycosylation. Selection of tri-GalNAc insulin was an obvious choice, because three GalNAc moieties are considered as most optimal for interaction with ASGPR receptor [24].
It was necessary to prepare tri-GalNAcB1-insulin in three independent reaction batches to ensure sufficient quantity for all biological assays.

The bioactivity of tri-GalNAcB1-insulin derivate was first tested in insulin tolerance test (ITT) in mice, where it showed similar activity (lowering of blood glucose) as human insulin, but at 4 times higher dose. We considered this result as logical because tri-GalNAcB1-insulin derivate is about 4-tomes less potent than human insulin in binding to IR-B. These experiments were done by Dr. Lenka Žáková from J. Jiráček's laboratory. Data are not shown.

Human insulin and tri-GalNAcB1-insulin were injected to male mice and after a short time delay samples of liver tissue and eWAT tissue were taken and immediately deep frozen (Methods). I have not participated in these experiments that were performed by Dr. Martina Chrudinová from J. Jiráček's laboratory.

For assessment of liver tissue selectivity of tri-GalNAcB1-insulin we tested level of activation (phosphorylation) of insulin receptor (IR) and Akt and Erk proteins that belong to IR signalling cascade by Western-blotting and using antibodies against phosphorylated forms of proteins. The results were compared to effects of human insulin and saline. The hypothesis was

that tri-GalNAc moieties in insulin will help to direct the conjugate to liver cells faster than human insulin by their specific interaction with ASGPR receptor that is exclusively expressed on the surface of hepatocytes. Similar effect was observed in the case of GalNac-modified siRNAs, which are successfully used for enhanced transport of therapeutic siRNAs to liver [24]. This mechanism is different from targeting liver with enhanced IR-B binding specificity of insulin analogues like LZ-162 prepared in the laboratory of Dr. Jiráček (see in Introduction and in [37]). The last data from Dr. Jiráček's show that LZ-162 in more active in liver (contains exclusively IR-B while peripheral tissues contains different proportions of Ir-A and IR-B, see in Introduction) than human insulin after injection to mice in the same experimental setup as used in this diploma thesis (non-published data). The moderate IR-B specificity of tri-GlaNacB1-insulin could be helpful in preferential transport of the conjugate to liver.

For injection of tri-GalNacB1-insulin we used 4-times higher dose (8 U/kg, one U is 6 nmol of derivate) than the dose of human insulin (2 U/kg). This ratio reflects the difference in binding affinities of both hormones for IR-B.

The Western-blotting was conducted on mice tissues with high IR-B content (liver, 95% IR-B) and higher IR-A (eWAT, 70% IR-B). The tissue samples were taken in a short delay after i.v. injection which is sufficient for a selective activation of IR-B in these tissues (our unpublished data with LZ-162).

The primary antibodies against autophosphorylated IR do not recognize difference between IR-A, IR-B or even IGF-1R due to high similarities of their tyrosine-kinases. However, IGF-1R is not abundant in these tissues (according to mRNA analyses done in the laboratory of Dr. Jiráček, not shown).

Unfortunately, the results from eWAT tissues were of insufficient quality (Figure 28), and the statistical evaluation of the data (not shown) did not provide any meaningful information. Therefore, our primary source of information on the biological activity of tri-GalNAcB1-insulin was the analysis of liver tissues (Figure 27). This does not undermine the main conclusions of this thesis, as the primary goal of this work was to develop an analogue with higher specificity towards IR-B, which is predominantly expressed in liver tissue.

Statistical analysis of samples from mouse livers (Figure 29) showed that human insulin is more effective in activating IR and Akt in the liver following intravenous injection than tri-GalNAcB1-insulin. This was observed despite the dose of the glycosylated analogue being adjusted for its IR-B binding affinity (in comparison to human insulin) and the inclusion of liver-targeting GalNAc groups. This is a particularly interesting result, especially considering the successful liver-targeting achieved with GalNAc-siRNAs.

The effects of saline, human insulin, and tri-GalNAcB1-insulin on Erk activation were identical. We attribute this lack of difference to the short time of tissue sampling (approximately 1 minute after injection), which was likely insufficient to observe effects on Erk phosphorylation, as this occurs further downstream in the insulin receptor signaling cascade.

We can only speculate that the conjugate is indeed selectively targeted to the liver through the ASGPR receptor. However, this receptor is primarily responsible for protein clearance from plasma and plays a key role in the transport of proteins into endosomes within hepatocytes (as described in Figure 7 of the Introduction). This phenomenon might have led to the glycosylated analogue being internalized via interaction with ASGPR, transported into endosomes, and subsequently degraded rather than binding to IR on the cell surface. This could explain the reduced bioactivity of the glycosylated analogue compared to human insulin.

A potential solution to this problem could involve the use of a cleavable linker between the insulin and the GalNAc part of the molecule, such as a linker containing a pair of basic residues for non-specific cleavage by a peptidase. Similar strategies are employed in clinically successful drug-antibody conjugates [38]. Such a linker would enable enzymatic cleavage after binding to the ASGPR receptor on the surface of hepatic cells, allowing the released insulin to activate the insulin receptor on the cell surface.

Interestingly, the hypothesis of tri-GalNAcB1-insulin transport via ASGPR to hepatic cells was recently supported by personal communication with Dr. Alexander N. Zaykov from Novo Nordisk Research Center Indianapolis, Indianapolis, IN, USA, who conducted a similar experiment with NAc-galactosylated insulins in the context of unpublished industrial research. His findings, which were consistent with ours, suggested that targeting insulin to ASGPR enhances clearance from circulation to the liver, but also increases endocytosis of the conjugate. This, in turn, leads to reduced activation of the insulin receptor.

6. Conclusion

In this diploma thesis, we successfully prepared four new NAc-galactosylated insulin derivatives, tested their in vitro binding affinities toward isoforms of the insulin receptor, and investigated the ability of the selected compound to activate insulin receptors in mouse tissues. Although we did not observe liver-specific effects of tri-GalNAcB1-insulin compared to human insulin, we optimized synthetic procedures and gained valuable insights into the biological properties of NAc-galactosylated insulin derivatives. The data will be included to a large study that is currently running in Dr. Jiráček laboratory and published later on.

7. References

1. Labster. Insulin Structure. <https://theory.labster.com/insulin-structure/> [21. 10. 2024]
2. Kurtzhals, P.; Nishimura, E.; Haahr, H.; et al.: Commemorating insulin's centennial: engineering insulin pharmacology towards physiology. *Trends Pharmacol. Sci*. **42**:8, 620–639 (2021). <https://www.sciencedirect.com/science/article/pii/S0165614721001088> [21. 10. 2024]
3. Panasevich, S., Lindgren, C., Kere, J., et al. Interaction between early maternal smoking and variants in TNF and GSTP1 in childhood wheezing. *Clinical & Experimental Allergy*. 2010, **40**(3), 458-467 https://doi.org/10.1111/j.1365-2222.2010.03452.x
4. Herring, R., Jones, R. H., Russell-Jones, D. L. Hepatoselectivity and the evolution of insulin. *Diabetes, Obesity and Metabolism*. 2014, **16**(1), 1-8. https://doi.org/10.1111/dom.12117.
5. Suckale, J., Solimena, M. The insulin secretory granule as a signaling hub. *Trends in Endocrinology and Metabolism*. 2010, **21**(10), 599-609 https://doi.org/10.1016/j.tem.2010.06.003
6. Steiner, D. F., Chan, S. J., Welsh, J. M., Kwok, S. C. Structure and evolution of the insulin gene. *Annual Review of Genetics*. 1985, **19**, 463-484. https://doi.org/10.1146/annurev.ge.19.120185.002335
7. Belfiore, A., Malaguarnera, R., Vella, V., et al. Insulin Receptor Isoforms in Physiology and Disease: An Updated View. *Endocrine Reviews*. 2017, **38**(5), 379-431. https://doi.org/10.1210/er.2017-00034.
8. Herring, R., Jones, R. H., Russell-Jones, D. L. Hepatoselectivity and the evolution of insulin. *Diabetes, Obesity and Metabolism*. 2014, **16**(1), 1-8. https://doi.org/10.1111/dom.12117.
9. Petersen, M. C., Shulman, G. I. Mechanisms of Insulin Action and Insulin Resistance. *Physiological Reviews*. 2018, **98**(4), 2133-2223. https://doi.org/10.1152/physrev.00063.2017.
10. Advanced Cardioprimary. Diabetes Management [online]. [21. 10. 2024]. Accessed: https://www.advancedcardioprimary.com/primary-care-services/chronic-conditions-management/diabetes-management/
11. Saltiel, A. R. Insulin signaling in health and disease. *Journal of Clinical Investigation*. 2021, **131**(1), e142241. https://doi.org/10.1172/JCI142241.
12. Cell Signaling Technology**.** Insulin Receptor Signaling Pathway. *Cell Signaling Technology* [online]. 2024 [21. 10. 2024]. Accesed: https://www.cellsignal.com/pathways/insulin-receptor-signaling-pathway.
13. Belfiore, A., Malaguarnera, R., Vella, V., et al. Insulin Receptor Isoforms in Physiology and Disease: An Updated View. *Endocrine Reviews*. 2017, **38**(5), 379-431. https://doi.org/10.1210/er.2017-00073
14. Jiráček, J., Žáková, L. Structural Perspectives of Insulin Receptor Isoform-Selective Insulin Analogs. *Frontiers in Endocrinology (Lausanne)*. 2017, **8**, 167. https://doi.org/10.3389/fendo.2017.00167
15. Galal, M. A., Alouch, S. S., Alsultan, B. S., et al. Insulin Receptor Isoforms and Insulin Growth Factor-like Receptors: Implications in Cell Signaling, Carcinogenesis, and Chemoresistance. *International Journal of Molecular Sciences*. 2023, **24**(19), 15006. https://doi.org/10.3390/ijms241915006
16. Science Photo Library**.** Insulin structure. [online]. 2024 [21. 10. 2024]. Accesed: https://www.sciencephoto.com/media/1045816/view.

17. Kurtzhals, P., Nishimura, E., Haahr, H., et al. Commemorating insulin's centennial: engineering insulin pharmacology towards physiology. *Trends in Pharmacological Sciences*. 2021, **42**(8), 620-639. https://doi.org/10.1016/j.tips.2021.05.005
18. Perkins, B. A., Sherr, J. L., Mathieu, C. Type 1 diabetes glycemic management: Insulin therapy, glucose monitoring, and automation. *Science*. 2021, **373**(6554), 522-527. https://doi.org/10.1126/science.abg4502
19. Kurtzhals, P., Nishimura, E., Haahr, H., et al. Commemorating insulin's centennial: engineering insulin pharmacology towards physiology. *Trends in Pharmacological Sciences*. 2021, **42**(8), 620-639. https://doi.org/10.1016/j.tips.2021.05.005
20. Craft, S., Raman, R., Chow, T. W., et al. Safety, Efficacy, and Feasibility of Intranasal Insulin for the Treatment of Mild Cognitive Impairment and Alzheimer Disease Dementia: A Randomized Clinical Trial. *JAMA Neurology*. 2020, **77**(9), 1099-1109. https://doi.org/10.1001/jamaneurol.2020.1840
21. Vienberg, S. G., Bouman, S. D., Sørensen, H., et al. Receptor-isoform-selective insulin analogues give tissue-preferential effects. *Biochemical Journal*. 2011, **3**, 301-308. https://doi.org/10.1042/BJ20110880
22. Zaykov, A. N., Mayer, J. P., DiMarchi, R. D. Pursuit of a perfect insulin. *Nature Reviews Drug Discovery*. 2016, **15**, 425-439. https://doi.org/10.1038/nrd.2015.36
23. Gallagher, E. J., LeRoith, D. Hyperinsulinaemia in cancer. *Nature Reviews Cancer*. 2020, **20**(11), 629-644. https://doi.org/10.1038/s41568-020-0295-5
24. Springer, A. D., Dowdy, S. F. GalNAc-siRNA Conjugates: Leading the Way for Delivery of RNAi Therapeutics. *Nucleic Acid Ther*. 2018;**28**(3):109-118. https://doi.org/10.1089/nat.2018.0736
25. Viková, J., Mitrová, K., Halamová, T., et al. Rational steering of insulin binding specificity by intra-chain chemical crosslinking. *Biochemical Journal.* 2016, **3**(14), 2035-2047. https://doi.org/10.1042/BJ20160132.
26. Sell, C., Dumenil, G., Deveaud, C., Miura, M., Coppola, D., DeAngelis, T., Rubin, R., Efstratiadis, A., & Baserga, R. (1994). Effect of a null mutation of the insulin-like growth factor I receptor gene on growth and transformation of mouse embryo fibroblasts. *Molecular and Cellular Biology, 14*(6), 3604–3612. https://doi.org/10.1128/mcb.14.6.3604-3612.1994
27. Frasca, F., Pandini, G., Scalia, P., Sciacca, L., Mineo, R., Costantino, A., Goldfine, I. D., Belfiore, A., & Vigneri, R. (1999). Insulin receptor isoform A, a newly recognized, high-affinity insulin-like growth factor II receptor in fetal and cancer cells. *Molecular and Cellular Biology,* **19** (5), 3278–3288. https://doi.org/10.1128/MCB.19.5.3278
28. Asai, S., Žáková, L., Selicharová, I., Marek, A., & Jiráček, J. (2021). A radioligand receptor binding assay for measuring insulin secreted by MIN6 cells after stimulation with glucose, arginine, ornithine, dopamine, and serotonin. *Analytical and Bioanalytical Chemistry, 413*(21), 5353–5364. https://doi.org/10.1007/s00216-021-03423-3
29. Záková, L., Kletvíková, E., Lepšík, M., Collinsová, M., Watson, C. J., Turkenburg, J. P., Jiráček, J., & Brzozowski, A. M. (2014). Human insulin analogues modified at the B26 site reveal a hormone conformation that is undetected in the receptor complex. *Acta Crystallographica Section D: Biological Crystallography,* **70**, 3054–3068. https://doi.org/10.1107/S1399004714017775
30. Furman, B. L. (2015). Streptozotocin-induced diabetic models in mice and rats. *Current Protocols in Pharmacology,* **70**(1), 5.47.1–5.47.20. https://doi.org/10.1002/0471141755.ph0547s70
31. Bradford, M. M. (1976). A rapid and sensitive method for the quantitation of microgram quantities of protein utilizing the principle of protein-dye binding. *Analytical Biochemistry, 72*(1-2), 248–254. https://doi.org/10.1016/0003-2697(76) 90527-3

32. Kolb, H. C., Finn, M. G., & Sharpless, K. B. (2001). Click chemistry: Diverse chemical function from a few good reactions. *Angewandte Chemie International Edition, 40*(11), 2004–2021. https://doi.org/10.1002/1521-3773(20010601)
33. Tornøe, C. W., Christensen, C., & Meldal, M. (2002). Peptidotriazoles on solid phase: [1,2,3]-triazoles by regiospecific copper(I)-catalyzed 1,3-dipolar cycloadditions of terminal alkynes to azides. *The Journal of Organic Chemistry,* **67**(9), 3057–3064. https://doi.org/10.1021/jo011148j
34. Kurtzhals, P., von Scholten, B. J., Kreiner, F. F., & Gough, S. C. L. (2021). Insulin at 100: Still central in protein-based therapy for chronic disease. *Nature Reviews Endocrinology, 18*(8), 453–466. https://doi.org/10.1038/s43856-021-00004-4
35. Østergaard, M., Mishra, N. K., & Jensen, K. J. (2020). The ABC of insulin: The organic chemistry of a small protein. *Chemistry - A European Journal, 26*(23), 5053–5062. https://doi.org/10.1002/chem.202000337
36. Chen, D., Disotuar, M. M., Xiong, X., Wang, Y., & Chou, D. H.-C. (2017). Selective N-terminal functionalization of native peptides and proteins. *Chemical Science, 8*(9), 6200–6205. https://doi.org/10.1039/c6sc04744k
37. Páníková, T., Mitrová, K., Halamová, T., et al. Insulin Analogues with Altered Insulin Receptor Isoform Binding Specificities and Enhanced Aggregation Stabilities. *J Med Chem*. 2021;64(19):14848-14859. https://doi.org/10.1021/acs.jmedchem.1c01388
38. Beck, A., Goetsch, L., Dumontet, C., & Corvaïa, N**.** (2017). Strategies and challenges for the next generation of antibody-drug conjugates. *Nature Reviews Drug Discovery, 16*(5), 315–337. https://doi.org/10.1038/nrd.2016.268